

NEUROPROTECTION FROM INDUCED GLUTAMATE EXCITOTOXICITY BY
CONUS BRUNNEUS CONOPEPTIDES IN A STROKE-RELATED MODEL

by

Rebecca A. Crouch

A Thesis Submitted to the Faculty of

The Charles E. Schmidt College of Science

In Partial Fulfillment of the Requirements for the Degree of

Master of Science

Florida Atlantic University

Boca Raton, FL

August 2013


NEUROPROTECTION FROM INDUCED GLUTAMATE EXCITOTOXICITY BY
CONUS BRUNNEUS CONOPEPTIDES IN A STROKE-RELATED MODEL

by

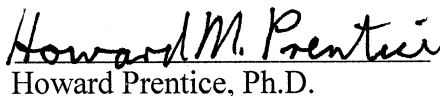
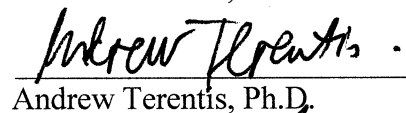
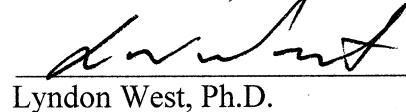
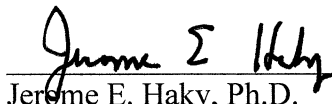
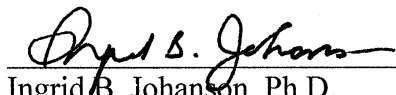
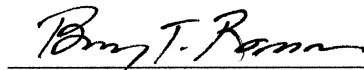
Rebecca A. Crouch

This thesis was prepared under the direction of the candidate's thesis advisor, Dr. Frank Mari, Department of Chemistry and Biochemistry, and has been approved by the members of her supervisory committee. It was submitted to the faculty of the Charles E. Schmidt College of Science and was accepted in partial fulfillment of the requirements for the degree of Master of Science.

SUPERVISORY COMMITTEE:



Frank Mari, Ph.D.
Thesis Advisor


Howard Prentice, Ph.D.
Andrew Terentis, Ph.D.
Lyndon West, Ph.D.
Jerome E. Haky, Ph.D.
Interim Chair, Department of Chemistry and Biochemistry
Ingrid B. Johanson, Ph.D.
Interim Dean, Charles E. Schmidt College of Science
Barry T. Rosson, Ph.D.
Dean, Graduate College

July 17, 2013
Date

ACKNOWLEDGEMENTS

I would like to express my appreciation to my supervisor, Dr. Frank Marí, for his guidance and assistance throughout my project. He was instrumental in providing me the tools and skills to carry out my experiments, as well as direction to the project overall.

I am also very thankful to Drs. Jang-Yen Wu and Howard M. Prentice for their support as collaborators and advisors, providing the facilities and technical knowledge and advice necessary to carry out the biological experiments.

I am most grateful to Dr. Jim Chen, a visiting scholar in Dr. Wu's laboratory, with whom I worked to carry out and interpret many of the biological experiments. Without his assistance and comments, the research could not have been completed.

I would also like to thank Drs. Lyndon West and Andrew Terentis for serving on my supervisory committee, for using their time and efforts to provide valuable comments on this thesis. Additionally, I would like to thank them for their support and advice throughout my graduate experience at Florida Atlantic University.

Furthermore, I would like to acknowledge my colleagues in Dr. Marí's research group, Alberto Padilla, Mickelene Hoggard, Mari Heghinian, and Alena Rodriguez, and in Dr. Wu's research group, Janet Menzie, Dr. Payam Gharibani, and Jigar Modi, for their kind support and helpful insights.

Lastly, I would like to thank my husband Dr. I. Victor Ogungbe for his unwavering encouragement and support.

ABSTRACT

Author: Rebecca A. Crouch
Title: Neuroprotection from Induced Glutamate Excitotoxicity by *Conus brunneus* Conopeptides in a Stroke-Related Model
Institution: Florida Atlantic University
Thesis Advisor: Dr. Frank Marí
Degree: Master of Science
Year: 2013

Cone snails are carnivorous marine mollusks, utilizing their neuropeptide-rich venom for prey capture. The venom of *Conus brunneus*, a wide-spread Eastern Pacific vermivore, has not been extensively studied. In the current work, peptides from the dissected venom were characterized and tested using preliminary bioassays. Six peptides (A-F) were isolated and tested. Three peptide identities were determined by comparison with previously reported data: bru9a (A), bru3a (F), and an α -conotoxin (E). Preliminary screening in a stroke-related model of induced glutamate excitotoxicity in primary neuronal cells and PC12 cell cultures indicated potential neuroprotective activity of peptide fractions A, D, and F. Further testing is necessary to determine and verify structure, activity, target, and mechanism of action of the promising peptides from *C. brunneus*, which may prove effective neuropharmacological agents to treat stroke.

NEUROPROTECTION FROM INDUCED GLUTAMATE EXCITOTOXICITY BY
CONUS BRUNNEUS CONOPEPTIDES IN A STROKE-RELATED MODEL

LIST OF TABLES	viii
LIST OF FIGURES	ix
1. INTRODUCTION	1
1.1. Cone snails and conopeptides	1
1.1.1 Molecular diversity of the venom	3
1.1.2 Neurotoxicity and pharmacology of venom.....	5
1.1.3 <i>Conus brunneus</i>	10
1.1.4 Current and future applications.....	12
1.2. Stroke	14
1.2.1. Symptoms and epidemiology	14
1.2.2. Biological effects – glutamate excitotoxicity and ER stress	16
1.2.3. Current stroke treatment options.....	20
1.3. The current stroke-related research model.....	23
2. MATERIALS AND METHODS.....	24
2.1. Materials	24

2.2. Conopeptide isolation and characterization	25
2.2.1. High-performance liquid chromatography (HPLC).....	25
2.2.1.1. Size-exclusion HPLC.....	25
2.2.1.2. Reverse-phase semi-preparative HPLC	26
2.2.1.3. Reverse-phase analytical HPLC	27
2.2.2. Matrix-assisted laser desorption/ionization-mass spectrometry (MALDI-MS)	27
2.2.3. Nuclear magnetic resonance (NMR) spectroscopy.....	28
2.2.4. Bioinformatics database comparison (Conoserver)	29
2.3. Cell cultures	29
2.3.1. Primary neuronal cell culture.....	29
2.3.2. PC12 cell culture	30
2.4. Glutamate excitotoxicity stroke-related model.....	31
2.4.1. Cell viability – ATP assay	31
2.4.2. Protein expression – Western blot analysis.....	32
3. RESULTS AND DISCUSSION	34
3.1. Conopeptide isolation and characterization.....	34
3.1.1. High-performance liquid chromatography (HPLC).....	34
3.1.1.1. Size-exclusion HPLC.....	34
3.1.1.2. Reverse-phase semi-preparative HPLC	36
3.1.1.3. Reverse-phase analytical HPLC	39
3.1.2. Matrix-assisted laser desorption/ionization-mass spec (MALDI-MS)	41

3.1.3. Nuclear magnetic resonance (NMR) spectroscopy	44
3.1.4. Bioinformatics database comparison (Conoserver)	51
3.2. Glutamate excitotoxicity stroke-related model.....	55
3.2.1. ATP assays – primary rat embryonic neuronal cell culture	55
3.2.2. ATP assays – PC12 cell culture	61
3.2.3. Western blot analysis	65
4. CONCLUSIONS.....	69
5. REFERENCES	71

LIST OF TABLES

Table 1. Peak table for <i>C. brunneus</i> crude venom size-exclusion HPLC separation.	36
Table 2. Relevant peak table for semi-prep HPLC separation of the major $\lambda = 280$ nm absorbance peak from the size-exclusion fraction of <i>C. brunneus</i>	38
Table 3. ^1H NMR chemical shifts of peptide fraction A (2533 Da) from <i>C. brunneus</i>	47
Table 4. ^1H NMR chemical shift values of bru9a from <i>C. brunneus</i> previously characterized in this laboratory. [13]	48
Table 5. Summary of <i>C. brunneus</i> peptide fraction identifying information.	51
Table 6. Conoserver search results for conopeptides with similar MW to PF B (3079 Da).	52
Table 7. Conoserver search results for conopeptides with similar MW to PF C (1885 Da).	53
Table 8. Conoserver search results for conopeptides with similar MW to PF D (2993 Da).	53
Table 9. Conoserver search results for conopeptides with similar MW to PF D (2621 Da).	54
Table 10. Conoserver search results for conopeptides with similar MW to PF E (1554 Da).	54

LIST OF FIGURES

Figure 1. Geographical localization of cone snails throughout the world.	1
Figure 2. Cartoon representation of the 2 general strategies of cone snail prey capture.	
A) Hook and line strategy, B) Net strategy. [4]	2
Figure 3. <i>Conus</i> conopeptide superfamilies, showing cysteine framework,	
pharmacological family, number of species, and characteristic PTMs. [3]	4
Figure 4. Organizational diagram of <i>Conus</i> peptides, showing the pharmacological	
family, gene superfamily, Cys framework, and molecular target. [7]	5
Figure 5. Organizational diagram of the M superfamily of conotoxins. [adapted, 9]	7
Figure 6. Mechanism by which the “motor cabal” blocks neuromuscular synaptic	
transmission. In order, 1) a presynaptic Ca^{2+} channel becomes blocked by	
an ω -conotoxin, 2) a postsynaptic nAChR becomes blocked by an α -	
conotoxin, and 3) a postsynaptic voltage-gated Na^{+} channel becomes	
blocked by a μ -conotoxin. [12]	8
Figure 7. Activity of both α -conotoxins and ψ -conotoxins to inhibit nAChRs. [12]	9
Figure 8. Ischemic versus hemorrhagic stroke.	16
Figure 9. Size-exclusion HPLC chromatogram of <i>C. brunneus</i> crude venom extract	
(absorbance at $\lambda = 220 \text{ nm}$).....	35
Figure 10. Size-exclusion HPLC chromatogram of <i>C. brunneus</i> crude venom extract	
(absorbance at $\lambda = 280 \text{ nm}$).....	35

Figure 11. Semi-prep HPLC chromatogram of <i>C. brunneus</i> fraction from size-exclusion (absorbance at $\lambda = 220$ nm).	37
Figure 12. Semi-prep HPLC chromatogram of <i>C. brunneus</i> fraction from size-exclusion (absorbance at $\lambda = 220$ nm), zoomed-in.	37
Figure 13. Semi-prep HPLC chromatogram of <i>C. brunneus</i> fraction from size-exclusion (absorbance at $\lambda = 280$ nm).	38
Figure 14. Semi-prep HPLC chromatogram of <i>C. brunneus</i> fraction from size-exclusion (absorbance at $\lambda = 280$ nm), zoomed-in.	38
Figure 15. Analytical HPLC chromatogram of <i>C. brunneus</i> peptide fraction A (absorbance at $\lambda = 220$ nm; R: 0.5).....	39
Figure 16. Analytical HPLC chromatogram of <i>C. brunneus</i> peptide fraction A (absorbance at $\lambda = 220$ nm; R: 1.0).....	40
Figure 17. Analytical HPLC chromatogram of <i>C. brunneus</i> peptide fraction A (absorbance at $\lambda = 220$ nm; R: 3.0).....	40
Figure 18. Analytical HPLC chromatogram of <i>C. brunneus</i> peptide fraction A (absorbance at $\lambda = 280$ nm).....	41
Figure 19. Representative MALDI-MS spectrum for peptide fraction A from <i>C. brunneus</i> . A mass peak of 2533 Da was observed.	42
Figure 20. Representative MALDI-MS spectrum for peptide fraction B from <i>C. brunneus</i> . A mass peak of 3079 Da was observed.	42
Figure 21. Representative MALDI-MS spectrum for peptide fraction C from <i>C. brunneus</i> . A mass peak of 1885 Da was observed.	43

Figure 22. Representative MALDI-MS spectrum for peptide fraction D from <i>C. brunneus</i> . Two mass peaks of 2993 and 2621 Da were observed.....	43
Figure 23. Representative MALDI-MS spectrum for peptide fraction E from <i>C. brunneus</i> . Two mass peaks of 2357 and 1554 Da were observed.....	44
Figure 24. Representative MALDI-MS spectrum for peptide fraction F from <i>C. brunneus</i> . A mass peak of 2127 Da was observed.	44
Figure 25. ¹ H NMR spectrum of peptide fraction A (2533 Da) from <i>C. brunneus</i>	45
Figure 26. TOCSY NMR spectrum of peptide fraction A (2533 Da) from <i>C. brunneus</i>	46
Figure 27. ¹ H NMR spectrum of peptide fraction C (1885 Da) from <i>C. brunneus</i>	49
Figure 28. TOCSY NMR spectrum of peptide fraction C (1885 Da) from <i>C. brunneus</i>	49
Figure 29. ¹ H NMR spectrum of peptide fraction F (2127 Da) from <i>C. brunneus</i>	50
Figure 30. TOCSY NMR spectrum of peptide fraction F (2127 Da) from <i>C. brunneus</i>	50
Figure 31. Comparison of the effects of conopeptide fractions A and B vs. taurine on rat primary neuronal cells under induced glutamate excitotoxicity. The approximate peptide fraction concentrations were: PF A (29.720 µg/mL), PF A (100X diluted: 0.2972 µg/mL), PF B (1.9444 µg/mL), and PF B (100X diluted: 0.0194 µg/mL). All the results shown are from wells that contained cells, except where noted (n=3).	56

Figure 32. ATP assay of Tau and Glu controls in primary neuronal cells. All the results shown are from wells that contained cells, except where noted (n=3).....	57
Figure 33. Summary of the ATP assay results for Tau and peptide fractions A-D neuroprotective activity against glutamate insult in primary neuronal cells. The approximate concentrations of the peptide fractions were: A (26.75 µg/mL), B (1.75 µg/mL), C (1.75 µg/mL), D (0.75 µg/mL); and, diluted peptide fractions: A (10X diluted: 2.675 µg/mL), B (10X diluted: 0.175 µg/mL), C (10X diluted: 0.175 µg/mL), and D (10X diluted: 0.075 µg/mL) All the results shown are from wells that contained cells (n=3).....	59
Figure 34. Summary of assay results of Tau and peptide fractions A-F. The approximate concentrations of the peptide fractions were: A (13.375 µg/mL), B (0.875 µg/mL), C (0.875 µg/mL), D (0.375 µg/mL), E (0.500 µg/mL), and F (5.625 µg/mL) neuroprotective activity against glutamate insult in primary, with Tau only and Glu only controls. All the results shown are from wells that contained cells (n=3).....	61
Figure 35. ATP assay of Tau and Glu controls in PC12 cells. The concentration of Tau was 10 mM. All the results shown are from wells that contained undifferentiated PC12 cells (2.8×10^5 cells/well).	62
Figure 36. ATP assay to determine the optimum concentration and pre-treatment time of Tau for future use as the positive control in PC12 cell tests	

(n=3). All the results shown are from wells that contained undifferentiated PC12 cells (2.8×10^5 cells/well).	63
Figure 37. ATP assay to determine the optimum concentration and pre-treatment time of Tau for future use as the positive control in PC12 cell tests, in terms of cell viability (n=3). All the results shown are from wells that contained undifferentiated PC12 cells (2.8×10^5 cells/well).	64
Figure 38. ATP assay of peptide fractions against glutamate insult in PC12 cells. For all of the peptide fraction tests, Glu (10 mM) was used. The peptide fraction concentrations were: PF A (53.50 $\mu\text{g/mL}$), PF B (3.50 $\mu\text{g/mL}$), PF C (3.50 $\mu\text{g/mL}$), PF D (1.50 $\mu\text{g/mL}$), PF E (2.0 $\mu\text{g/mL}$), and PF F (22.5 $\mu\text{g/mL}$). All the results shown are from wells that contained undifferentiated PC12 cells (2.8×10^5 cells/well) (n=3).	65
Figure 39. Western blot of the pro-survival markers Akt and Bcl-2 in PC12 cells pre-treated with peptide fractions and exposed to Glu.	66
Figure 40. Western blot of several markers of ER stress and apoptosis in rat primary neuronal cells pre-treated with peptide fractions and exposed to Glu. A) Pro-survival Bcl-2, and pro-apoptotic calpain and caspase-12. B) GAPDH internal control and UPR-upregulated ER chaperone GRP78.	67

1. INTRODUCTION

1.1. Cone snails and conopeptides

Cone snails are venomous marine mollusks that live mainly in tropical waters, especially on or near coral reefs, including the tropical waters in the Atlantic Ocean, the Panamic region (tropical west coast of the Americas), and the Indo-Pacific region [1,2]. The geographical locations in which cone snails have been found to dwell are shown below in Figure 1.



Figure 1. Geographical localization of cone snails throughout the world.

Cone snails are classified within the genus *Conus*, subfamily Coninae, family Conidae, and superfamily Conoidea. The number of *Conus* species has been approximated at 700 [3]. As slow-moving animals, these gastropods have developed sophisticated prey capture techniques in order to survive.

While all cone snails are predatory carnivores, each specializes in capturing and feeding on just one of the following: fish (piscivores), worms (vermivores), or other mollusks (molluscivores). The snails, in general, use 1 of 2 different strategies to paralyze and ingest their prey, the hook and line strategy or the net strategy, shown below in Figure 2 [4]. To date, only some fish-hunting cone snails have been observed using the net strategy. Both strategies employ the cone snails' characteristic venom, which contains a highly complex and specific mixture of specialized peptides and proteins called conopeptides and conoproteins, respectively. Researchers have mainly been interested in investigating the conopeptides, which have been shown to play key roles in the neurophysiological effects observed in the cone snails' prey when they are injected with or surrounded by the venom.

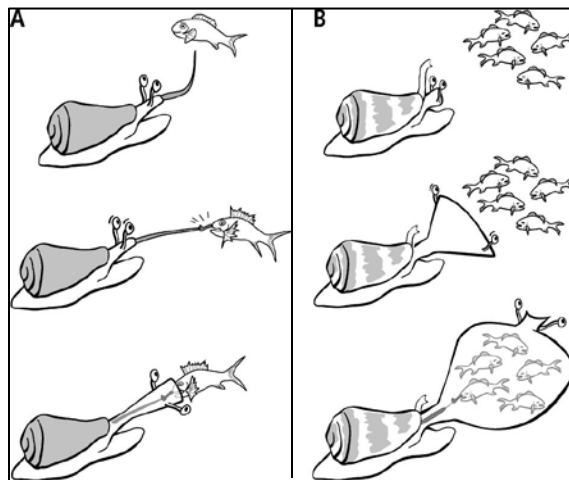


Figure 2. Cartoon representation of the 2 general strategies of cone snail prey capture.

A) Hook and line strategy, B) Net strategy. [4]

In the hook and line strategy, a snail uses its proboscis (loaded with a single disposable radula tooth from its radula sac) to harpoon its prey. At this point, venom is

ejected from the venom bulb through the venom duct and proboscis. The radula tooth then acts as a hypodermic needle to inject the prey with a venom cocktail of conopeptides that immobilizes it almost instantaneously. Once immobilized, it is engulfed by the cone snail [4]. Conversely, some snails are able to use a net strategy to capture their prey (fish-eaters only). In this strategy, a cone snail first releases conopeptides that have a calming effect on the fish as a result of sensory deadening. Next, the snail captures the fish within its highly stretchable rostrum, and finally injects them with paralyzing conopeptides and ingests them [4].

1.1.1 Molecular diversity of the venom

As mentioned above, cone snail venom is composed of many components, including conopeptides, with 1000-8000 specific peptides depending upon the species of snail [3]. This venom is used by the snails for more than just prey capture; it is also used for defense and competition. Using its venom, a cone snail is able to interact with its environment in a manner much like the interactions among different bacteria (quorum sensing) or insects (pheromones), in that the communication among individuals takes place via a chemical signal. No matter the situation, the snails are able to use their venom effectively due to the biodiversity of conopeptides and other molecules it contains.

The term conopeptide actually includes several different groups of peptides known as conotoxins, conopressins, contryphans, and others [5]. The most studied group of conopeptides are the conotoxins, due to their potent and selective activities at specific axonal or post-synaptic target at neuromuscular junctions. The three main classes of targets are voltage-gated or ligand-gated ion channels and G-protein coupled receptors.

Each conotoxin is unique in its 3-D structure and neurophysiological activity. This is due to a wide range of biodiversity, resulting not only from the hypervariability of the peptide amino acid sequence, but also from diverse patterns of cysteine groups and disulfide bond connectivity, as well as other post-translational modifications (PTMs) that the short peptides (6-40 amino acids) undergo [6]. Such PTMs include γ -carboxylation of glutamate, epimerization of L- to D-amino acids, bromination of tryptophan, sulfation of tyrosine, *O*-glycosylation, hydroxylation of proline, C-terminal amidation, proteolysis, and disulfide bond formation [3]. The conotoxins with known sequence and structure have been organized into a classification system of superfamilies, based on their common cysteine frameworks (Figure 3) [3], even while their molecular targets and functions may be quite different. Superfamilies A, M, and O are the most studied and most populous. The peptides may be classified further, depending on their general neurological target; these will be discussed in the next section and are included in a more detailed organizational diagram shown below in Figure 4 [7].

Superfamily	Cysteine Framework	Family	Species	Clades	Diet	PTMs
A	I, II, IV, XIV	α, κ, ρ	43	E, I, II, III, V, VI, VII, X, XII, XIV, XV, XVII	V, M, P	O, *, γ , G, Z, Ys
D	XX	α	6	XII	V	O, γ
I1	VI/VII, XI	ι	11	E, I, V, X, XIV, XVII	V, M, P	O, BrW, *, D, γ
I2	XI, XII	κ	17	I, V, VI, X, XII, XIII, XVII	V, M, P	O, *, γ
I3	VI/VII, XI		3	XIV	V	
J	XIV	κ	2	IX	V	*
L	XIV	α	2	E	V, P	
M	III, IV, VI/VII, IX, XVI	$\alpha, \iota, \kappa, \mu$	28	E, I, II, III, IV, V, VI, VII, X, XII, XIV, XVI, XVII	V, M, P	O, *, D
O1	VI/VII, XII	$\delta, \gamma, \kappa, \mu O, \omega$	53	E, I, II, III, V, VI, VII, IX, X, XI, XII, XIII, XIV, XV, XVI, XVII	V, M, P	O, BrW, *, γ
O2	VI/VII, XV	γ	15	I, V, VI, VII, X, XII, XIII, XIV, XVI	V, M, P	O, BrW, *, γ
O3	VI/VII		6	V, VII, XIV, XVI	V, M, P	
P	IX		6	V, X, XVII	V, M	*, γ
S	VIII	α, σ	6	I, II, V, XIV	V, M, P	O, BrW, *, γ
T	I, V, X, XVI	χ, ε, μ	24	E, II, III, V, VI, VII, X, XII, XIII, XIV, XVI, XVII	V, M, P	O, BrW, *, γ , G, Z
V	XV		2	XIII	V	*
Y	XVII		1	XIV	V	O

E, early clade; P, fish; M, molluscs; V, worms; *, C-terminal amidation; O, hydroproline; BrW, bromotryptophane; D, D-amino acid; γ , γ -carboxyglutamate; γ -Val, γ -hydroxyvaline; G, glycosylation; Z, pyroglutamate; Ys, sulfotyrosine.

Figure 3. *Conus* conopeptide superfamilies, showing cysteine framework, pharmacological family, number of species, and characteristic PTMs. [3]

1.1.2 Neurotoxicity and pharmacology of venom

As mentioned above, the activities of several conopeptides have been linked to their specific interaction with certain ion channels or G-protein coupled receptors (GPCRs) at neuronal or neuromuscular synapses which disrupts synaptic signaling and causes different forms of paralysis [3,8]. The general targets of each group of conopeptides are shown below in Figure 4.

Pharmacological family	Membrane receptor family and binding mode	# Mature conotoxins	Gene superfamily	Cysteine framework	# Species
α (alpha)	Nicotinic acetylcholine receptors (nAChR)	55	A, D, L, M, S	I, II, III, IV, VIII, XIV, XX	26
χ (chi)	Neuronal noradrenaline transporter	4	T	X	1
δ (delta)	Voltage-gated Na channels (agonist; delayed inactivation)	18	O1	VI/VII	13
ϵ (epsilon)	Presynaptic Ca channels or G protein-coupled presynaptic receptors	1	T	V	1
γ (gamma)	Neuronal pacemaker cation currents (inward cation current)	4	O1, O2	VI/VII	4
ι (iota)	Voltage-gated Na channels (agonist; no delay inactivation)	2	I1, M	III, XI	2
κ (kappa)	Voltage-gated K channels (blocker)	8	A, I2, J, M, O1	III, IV, VI/VII, XI, XIV	6
μ (mu)	Voltage-gated Na channels (blocker)	23	M, O1, T	III, IV, V, VI/VII	13
ω (omega)	Voltage-gated Ca channels (blocker)	31	O1	VI/VII	10
ρ (rho)	Alpha1-adrenoceptors (GPCR)	1	A	I	1
σ (sigma)	Serotonin-gated ion channels (GPCR)	1	S	VIII	1

Figure 4. Organizational diagram of *Conus* peptides, showing the pharmacological family, gene superfamily, Cys framework, and molecular target. [7]

As shown in Figure 4, there are several many conotoxins (55) in 5 different superfamilies that target nicotinic acetylcholine receptors (nAChRs). While both α - and α A-conotoxins are competitive inhibitors of nAChRs, the ψ -conotoxins are noncompetitive inhibitors. The κ conotoxins (including κ A-, κ -, and κ M-conotoxins) target voltage-gated K^+ , the δ - and μ -conotoxins target voltage-gated Na^+ channels, and

the ω -conotoxins target voltage-gated Ca^{2+} channels. The κ -conotoxins and κA -conotoxins act by blocking voltage-gated K^{+} channels, while the μ -conotoxins and μO -conotoxins act by blocking voltage-gated Na^{+} channels. Meanwhile, the ω -conotoxins act by blocking voltage-sensitive Ca^{2+} channels. Interestingly, δ -conotoxins act by delaying the inactivation of voltage-sensitive Na^{+} channels.

Contrary to the simplified diagram shown in Figure 4, the M superfamily can be divided into several more subfamilies. As of 2010, there were 5 families, M-1 – M-5 [9]. All M superfamily conotoxins have the same cysteine motif in their amino acid sequence, but not all have the same disulfide bonding pattern. M-4's and M-5's (with identical disulfide bonding patterns) make up the maxi-M's, including the well-known μ -, κM -, and ψ -conotoxins. M-1 – M-3's are called the mini-M's. While maxi-M's have been found primarily in fish-hunting cone snails, mini-M's have mainly been found in non-fish-hunters. The disulfide bonding patterns of M-1's and M-2's are unique. The first known mini-M was mr3a from *Conus marmoreus* (an M-2 that has a distinctive “triple-turn” backbone) [10]. Also from *C. marmoreus* is the mini-M mr3b. Several other mini-M's have been isolated from *Conus textile*, including tx3a (an M-1 that also has a “triple-turn” motif), tx3b, and tx3c. The mini-M's are, structurally, extremely constrained by the nature of their short amino acid sequences (17-20) and 3 disulfide bridges. When tested in mice, each of the 5 mini-M's mentioned above caused one or more behavior effects including scratching, hyperactivity, circular motion, and/or barrel rolling [11].

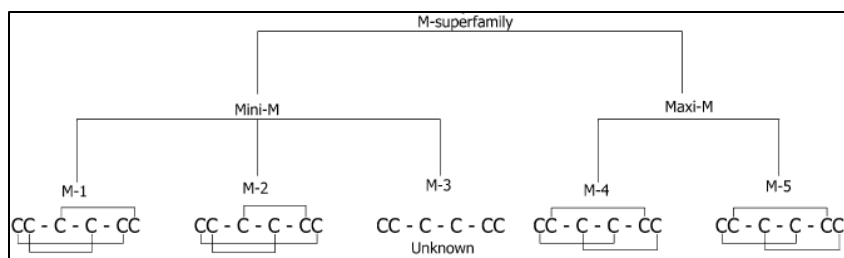


Figure 5. Organizational diagram of the M superfamily of conotoxins. [adapted, 9]

To detail more specifically how the conotoxins coordinate their activities upon injection into a cone snail's prey in order to bring about the paralytic effects observed in nature, a more complete visual picture must be drawn of the spatiotemporal separation of each of the steps that lead to total paralysis. In a basic model, there are 2 main stages, with the first being an almost instantaneous immobilization within 2 seconds of injection and the second being a complete block of neuromuscular function (irreversible paralysis) within 20 seconds of injection. The first stage is required in order to observe the excitotoxic effects seen in nature (see Figure 2A above) – if the second stage alone is used, only a flaccid state of paralysis is observed. The key players in the first stage are collectively called the “lightning strike cabal” and consist at minimum of a δ -conotoxin that increases axonal sodium channel conductance and a κ -conotoxin that blocks potassium channels. In the absence of δ -conotoxin, sodium channels in the closed position will open normally when signaled, then will immediately shift into an inactive state, which blocks the channel pore, but when δ -conotoxin is present, it binds to the sodium channel so that the inactive state is inhibited and the channel is always open, producing a persistent current. Similarly, in the absence of κ -conotoxin, the potassium channel will open normally when signaled, allowing potassium ions to flow out of the cell; however, when κ -conotoxin is present, it binds to the pore of the potassium channel

and blocks potassium from flowing out. In addition, some other conotoxins are present in the “lightning strike cabal” that act to depolarize the neuronal cell membrane by causing sodium to flow inside and potassium to remain inside (makes cell interior more positive). The combined result is that the neuronal axons fire uncontrollably, making the prey unable to control its movements. The key players in the second stage of paralysis via cone snail venom are collectively called the “motor cabal” and consist of 4 groups of conotoxins that ultimately result in complete and irreversible immobilization of the prey. The 4 groups of conotoxins are ω -conotoxins that target presynaptic (axonal) calcium channels, α -conotoxins that target postsynaptic nAChRs, γ -conotoxins that target postsynaptic nAChRs at ion channels, and μ -conotoxins that target postsynaptic voltage-gated sodium channels in skeletal muscle cell membranes, shown in Figure 6. [12]

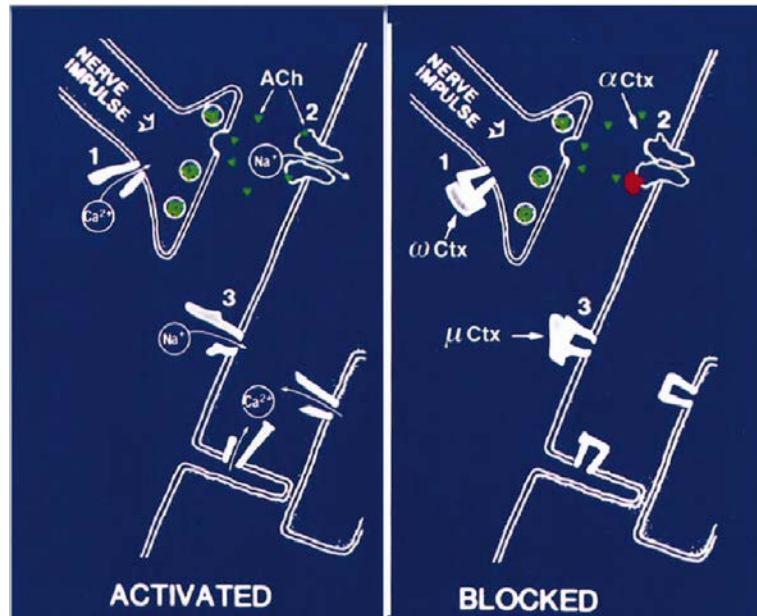


Figure 6. Mechanism by which the “motor cabal” blocks neuromuscular synaptic transmission. In order, 1) a presynaptic Ca^{2+} channel becomes blocked by an ω -

conotoxin, 2) a postsynaptic nAChR becomes blocked by an α -conotoxin, and 3) a postsynaptic voltage-gated Na^+ channel becomes blocked by a μ -conotoxin. [12]

Thus, while the activities of the conotoxins involved in the “lightning strike cabal” and the “motor cabal” may seem contradictory or counterproductive in some cases, they actually work synergistically to inhibit multiple targets, functioning together to give the result of total paralysis. The cone snails have also developed completely unrelated peptides (structurally) to obtain the same effect, so that there is overlap of activity of many conotoxins. One example is shown below in Figure 7, in which α -conotoxins and ψ -conotoxins bind in a different way to a nAChR to block its channel from allowing sodium ions to pass through [12].

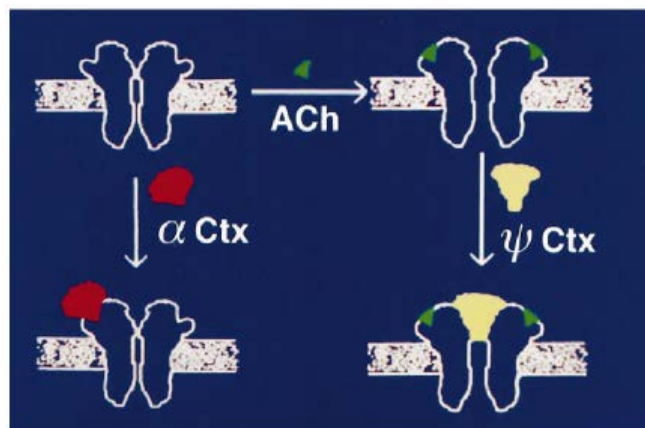


Figure 7. Activity of both α -conotoxins and ψ -conotoxins to inhibit nAChRs. [12]

Still, other conotoxins target 5-HT₃ (serotonin) receptors (σ -conotoxins) or NE (norepinephrine) transporters (χ -conotoxins). Meanwhile, the contualkins target neuropeptide receptors, the conantokins target N-methyl-D-aspartate (NMDA) receptors, and conopressins target vasopressin receptors. Contualkins and conopressins are GPCR

agonists. Many of these conopeptides play a role in the calming effects (through sensory deadening) observed in the initial stage of the net strategy of prey capture [4].

1.1.3 *Conus brunneus*

The first specimen of *Conus brunneus* (“brown cone”) was described by Wood in 1828, dredged from a depth of 75 feet off of the Pacific coast of Gubernadora Island in Panama. It is a fairly common cone snail species that is found in intertidal to moderately deep waters throughout the Eastern Pacific Ocean, from the Gulf of California to Ecuador. *C. brunneus* is a worm-eating (vermivorous) snail that uses a hook and line strategy to capture mainly polychaete worms. The prey capture apparatus and technique of this cone snail were previously studied by this laboratory [13]. It was observed that the snail extends its proboscis until locating a worm, which it immediately harpoons with its radular tooth (containing two barbs) and injects with its venom which travels through its large, off-white to yellow venom duct from the venom bulb to the tip of the proboscis. The venom of this cone snail paralyzed the prey immediately, and the snail began pulling the worm towards its mouth using the radular tooth hooked into the worm’s flesh. Interestingly, the paralytic effects of the venom were observed to be localized and reversible, though it was not determined if this was due to a defense mechanism of the worm. The cone snails were rarely observed ingesting an entire worm and instead ingested only part of the worm, while the other part pinched off near the venom injection site and swam away with no lasting effects of the venom. Additionally, if a worm was able to escape from the cone snail’s grasp, the paralytic effects of the venom would wane, and the worm would eventually have complete freedom of motion again. Thus, it was

concluded that the effects of conopeptides isolated from *C. brunneus* may be reversible also, suggesting that they are likely capable of reversibly binding to specific target ion channels or receptors, and making them highly desirable as potential neuropharmaceuticals [13].

Several conopeptides have been isolated and characterized from the venom of *C. brunneus* in this laboratory. One of these was an α -conotoxin (MW: 2360 Da) which had the sequence TWD γ CCKNPACRNNHKDKCG (where γ is a post-translationally-modified γ -carboxyglutamate), consistent with an α -conotoxin from the A superfamily. The γ -carboxyglutamate has been found to bind Ca^{2+} and has been shown to be necessary for Ca-induced interactions with membrane surfaces, in addition to adding structural rigidity to the conopeptide itself [14-16]. This particular α -conotoxin is referred to as an $\alpha 4/7$ conotoxin due to its 4 non-Cys amino acids in the first loop and the 7 non-Cys amino acids in the second loop, with disulfide bonding pattern Cys1-Cys3 and Cys2-Cys4. As discussed above, α -conotoxins are known to competitively and selectively inhibit neuronal nicotinic acetylcholine receptors; however, the specific target of this α -conotoxin has not been determined.

Also discovered was a novel P superfamily conotoxin called bru9a. The 24-amino acid sequence was determined to be SCGGSCFGGCWOGCSCYARTCFRD (MW: 2534 Da), where O is a post-translationally-modified 4-hydroxyproline. The disulfide bond pattern was also determined: Cys2-Cys14, Cys6-Cys16, and Cys10-Cys21, consistent with the P superfamily pattern (I-IV, II-V, and III-VI), and forming a classic inhibitory cysteine knot motif. Since there are no adjacent Cys residues in P superfamily peptides, it

is thought that these conotoxins may display a great diversity of structure and function. The molecular target of this peptide is still unknown.

Additionally discovered were two novel mini-M conotoxins from the M superfamily called bru3a and bru3b. The sequence of the 18-amino acid peptide bru3a was determined to be CCRWPRCNVYLCGOCCOQ (MW: 2127 Da), where again each O is a post-translationally-modified 4-hydroxyproline. Meanwhile, bru3b was a 15-amino acid peptide with the sequence CCQAYCSRYHCLPCC (MW: 1746 Da). Both bru3a and bru3b contain 3 disulfide bonds, both of them in the pattern belonging to the M-2 subclass (I-VI, II-IV, III-V). The molecular targets of these mini-M conotoxins have yet to be determined.

As a side note, *C. brunneus* was also used in this laboratory as a test organism to develop a new bioassay that allows testing and comparison of venoms and peptides from various species, and even gives an indication of potential molecular targets, *in vivo* using the *D. melanogaster* giant fiber system [17].

1.1.4 Current and future applications

Since the discovery of conopeptides, their pharmacological potential has been the driving force behind their extensive study. To date, several conopeptides have gone through various phases of clinical testing, and some have made it all the way through clinical trials and are actually commercially available treatment options for certain neurophysiological conditions. Their appeal as drug candidates is enhanced by the fact that most have been shown to be highly selective for certain target receptors versus others in the same family [6].

A major advance in the treatment of neuropathic pain came with the discovery of the ω -conotoxin MVIIA, an N-type calcium channel blocker called ziconotide that was originally isolated from *Conus magus* by the Olivera group at the University of Utah [18]. Ziconotide was shown to be 10-100 times more potent than morphine, and it did not produce the same tolerance or addiction. In December 2004, this conotoxin was approved by the U.S. Food and Drug Administration to be marketed as a drug (called Prialt) that could be injected directly into the spinal cord via an intrathecal pump. During the same time frame, another conotoxin was being studied by the Livett group (at the University of Melbourne) that they originally isolated from *Conus victoriae* to be used to treat the same chronic neuropathic pain. This peptide called ACV1 (analgesic component of venom 1) had the same positive effects as Prialt but without the undesirable side effects including extremely high blood pressure, and with injection under the skin or into the muscle rather than directly into the spinal cord. This conotoxin entered Phase II clinical trials in 2007, but the trials were abandoned when it was determined that the concentration of peptide required for efficacious treatment was too high. For the past couple of years, the Craik group at the University of Queensland has been studying peptides from *Conus victoriae* which they have cyclized and which have shown even more powerful effects as pain relievers as a result of their increased stability [19,20].

Other examples include contulakin-G (an *O*-linked glycopeptide similar to endogenous neurotensin), originally isolated from *Conus geographus*, which has been studied as a treatment for intractable pain. Contulakin-G acts as an agonist of neurotensin receptors. This conopeptide entered Phase II clinical trials in 2006. Meanwhile, another

peptide called conantokin entered Phase I clinical trials in 2006 as a treatment for epilepsy. Both of these peptides act to calm down the neuronal circuitry.

As of yet, the targets of many conopeptides have not been determined. With 1000-8000 unique peptides in each of the 700+ *Conus* species, over 1 million neuroactive peptides could be characterized and studied for their pharmacological potential [3]. It has been suggested that the conopeptides present in cone snails could still find uses as therapeutics to treat a wide range of conditions and diseases. Several of these include anxiety disorders, Parkinson's disease, pain, muscle tension, hypertension, and cancer, which could be treated by specific α - or ψ -conotoxins that work as antagonists of neuronal and skeletal muscle nAChRs. Additionally, μ -conotoxins could be used as neuromuscular blocking agents, as local anesthetic/analgesic agents, or as neuro-protective agents due to their interaction with skeletal muscle sodium channels [21]. Other major diseases such as stroke could be treated with ω -conotoxins (act on calcium channels) or conantokins (act on NMDA receptors). And, κ -conotoxins have shown promise as treatments for hypertension, arrhythmia, and asthma by acting on potassium channels. Finally, conantokins may also help alleviate symptoms of epilepsy by acting on NMDA receptors. [22]

1.2. Stroke

1.2.1. Symptoms and epidemiology

Stroke is a condition characterized by the rapid deterioration of brain function due to a sudden decrease in the supply of blood (ie, glucose and oxygen) to the brain.

According to the American Heart Association [23], approximately 795,000 people in the

U.S. experience a stroke each year, with about 610,000 being first strokes and about 185,000 being recurrent strokes. This means that, on average, 1 person has a stroke every 40 seconds in the U.S. [23]. Statistics show that, out of all strokes, approximately 87% are ischemic (thrombotic or embolic), 10% are intracerebral hemorrhage, and 3% are subarachnoid hemorrhage strokes [24]. In 2005, stroke mortalities accounted for more than 5% of deaths in the U.S, making stroke the 3rd leading cause of death behind heart disease and cancer [23].

Fortunately, the number of deaths due to stroke decreased in the decade from 1995-2005 by 13.5%, with a decrease in the annual stroke death rate of 29.7% [25]. However, even though stroke death rates have been decreasing, approximately 15-30% of persons who do suffer a stroke are faced with permanent disabilities, with 20% requiring institutional care [26]. In particular, among ischemic stroke survivors aged ≥ 65 years, 50% had some hemiparesis (localized muscle weakness on one side of the body due to nerve damage), 30% required some assistance to walk, 26% required assistance in daily living activities, 19% had aphasia (difficulty understanding or formulating either written or oral language), 35% had symptoms of depression, and 26% were institutionalized in an adult-care facility [27]. Because 8-12% of ischemic strokes and 37-38% of hemorrhagic strokes result in death within 30 days in 45-64 year-old persons [28], there is still much work to be done to improve the treatment of stroke. Much can be done by first examining what happens to the brain during a stroke, and then devising novel therapeutic approaches to prevent strokes and treat stroke victims.

1.2.2. Biological effects – glutamate excitotoxicity and ER stress

As mentioned above, there are 3 main types of stroke: ischemic (due to lack of oxygen in brain tissue), intracerebral hemorrhage (due to bleeding in the interior of the brain tissue), and subarachnoid hemorrhage (due to bleeding in the space between the brain and the surrounding tissue) [29]. A diagram displaying general ischemic and hemorrhagic stroke is shown in Figure 8. In both cases, a lack of glucose and O₂ eventually lead to reduced protein synthesis and energy failure [30].

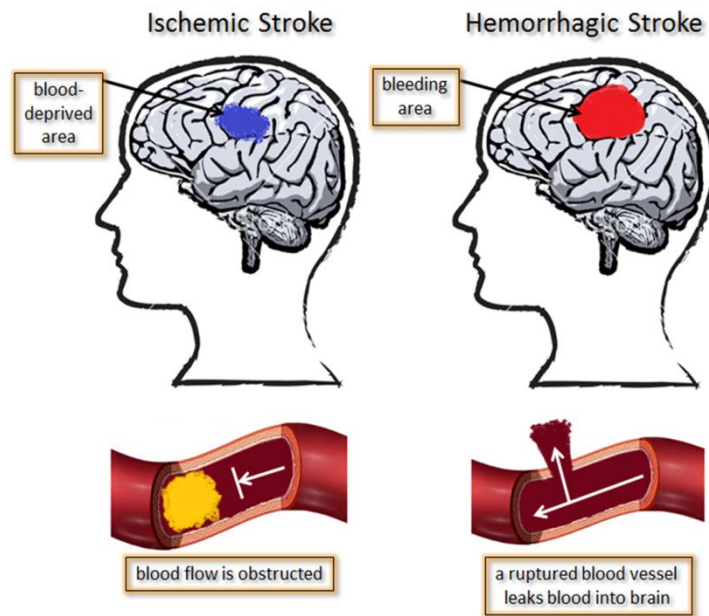


Figure 8. Ischemic versus hemorrhagic stroke.

On the molecular level, ischemia leads to an increase in the extracellular concentrations of excitatory amino acids, especially glutamate [31]. This increase may be due to one or both of the following: 1) increased release of glutamate from neuronal axons, and/or 2) reduced clearance of glutamate by glial transporters. Both of these would result from ATP depletion caused by the lack of glucose and O₂ in the affected

area, eventually making ATP-dependent active transport impossible. Due to the reduced capability of ATP-dependent ion pumps (including the extremely important Na^+/K^+ -ATPase) to operate, membrane depolarization results, and the neurons are unable to maintain normal transmembrane electrochemical gradients [32]. An influx of extracellular Ca^{2+} into the neurons through voltage-sensitive Ca^{2+} channels occurs, followed by the uncontrolled release of excitatory amino acids (ie, glutamate) into the extracellular space [33].

In times of normal neuronal functioning, small amounts of glutamate (the most prevalent excitatory neurotransmitter) are essential; however, at the excessive levels experienced during ischemia, glutamate becomes excitotoxic—poisonous—to the neurons [34]. Glutamate (whose exocytosis, as mentioned above, results from Ca^{2+} -induced stimulation of presynaptic axons) itself activates N-methyl-D-aspartic acid (NMDA) and other receptors, further stimulating Ca^{2+} influx into the neurons and perpetuating the cycle of glutamate release [35]. At the same time Ca^{2+} is flowing in, Na^+ and Cl^- ions are allowed to passively flow into the neurons, while K^+ ions also stay inside the cells (just as it occurs with conopeptides in the “lightning strike cabal”). Additional nonselective cation channels and acid-sensing ion channels add to the calcium ion imbalance [36,37]. All of these things lead to an influx in H_2O , resulting in cytotoxic edema and rapid cell death [38,39]. In addition, several Ca^{2+} -requiring enzymes (ie, proteases, lipases, nucleases, and kinases) become activated and carry out their destructive, catabolic functions which lead to cell death by degrading structural

components and circumventing the anabolic processes [40,41]. Finally, apoptosis occurs, leading to the loss of cognitive and motor function experienced by stroke victims.

Meanwhile, during an ischemic stroke, a high level of endoplasmic reticulum (ER) stress is also observed [42]. This can be due to a high level of protein misfolding and/or aggregation, which may be due to an insufficient amount of ER chaperones, such as GRP78 (glucose-regulated protein 78), one of the most abundant and best studied ER chaperones. As the site of protein synthesis and folding, the ER must function properly in order for the cell to survive. Specific proteins are essential for transmembrane electrochemical gradient regulation, intracellular Ca^{2+} homeostasis, and activation (or deactivation) of cell death pathways [43]. When, for any reason, proteins are not being folded properly, the ER stress response signaling pathways called the Unfolded Protein Response (UPR) are activated [44]. Several recent studies have highlighted the important role of ER stress response in the pathogenesis of neuronal cell injury during and after cerebral ischemia [45-47].

There are three main signaling pathways associated with the UPR. Each one is initiated by an ER-membrane-associated protein: 1) protein kinase R-like ER kinase (PERK), 2) inositol-requiring enzyme 1 (IRE1), and 3) activating transcription factor 6 (ATF6). These three proteins activate three distinct UPR signaling cascades [48-50]. It has been shown that cardiac ischemia induces all three of these pathways and their downstream targets [51,52], while the ER stress response in cerebral ischemia has not been well-studied.

While only the IRE1 and ATF6 pathways stimulate production of ER protein folding chaperones (such as GRP78), all three pathways stimulate production of a transcription factor called C/EBP homologous protein (CHOP) or growth arrest and DNA damage-inducible gene 153 (GADD153) [53-55]. CHOP/GADD153 is important, as it regulates the expression of several pro- or anti-apoptotic members of the Bcl-2 family of proteins. While it inhibits expression of the anti-apoptotic Bcl-2 [56], it induces expression of the pro-apoptotic Bim [57].

Although IRE1 in complex with certain proteins (ex: XBP1) has been shown to be anti-apoptotic, if it is overexpressed or complexed with other proteins (ex: TRAF2), apoptotic cell death results [49, 58, 59]. It may be that IRE1-XBP1 activity occurs during short-term ER stress, while IRE1-TRAF2 activity occurs during long-term ER stress. IRE1 also activates a protein called c-Jun N-terminal kinase (JNK) which regulates Bcl-2 family proteins (like CHOP/GADD153), suppressing the anti-apoptotic and enhancing the pro-apoptotic activities [60]. Thus, both JNK and CHOP/GADD153 eliminate the anti-apoptotic effects of Bcl-2, CHOP/GADD153 by blocking expression of Bcl-2, and JNK by phosphorylating it. It also activates the pro-apoptotic Bcl-2 family proteins Bax, Bak, and Bim. Thereby, a death signal is sent to the mitochondria, and cytochrome c is released, followed by caspase activation.

The PERK pathway also aids in cell survival during short-term ER stress by inhibiting protein translation and thereby decreasing the load of nascent proteins arriving at the ER needing to be folded. However, at the same time, PERK upregulates activating transcription factor 4 (ATF4), and ATF4, in turn, induces transcription of several genes

necessary to restore ER homeostasis. Yet, another protein ATF4 upregulates is the pro-apoptotic CHOP/GADD153. In addition, the PERK pathway can activate caspase-12, a key pro-apoptotic protein. Therefore, it seems that, with short-term ER stress, the anti-apoptotic and repair pathways are upregulated, enhancing the ER's protein folding capabilities and initiating the degradation of protein aggregates; however, as ER stress persists, the pro-apoptotic pathways take over and lead to apoptotic cell death [61].

1.2.3. Current stroke treatment options

Currently, only one FDA-approved treatment is available to patients suffering from an acute ischemic stroke. It is a thrombolytic agent called tissue plasminogen activator (tPA). Thrombolytic agents are administered intravenously in order to dissolve or break up a blood clot, and most are only administered within a certain time period of the onset of symptoms, 3 hours in the case of tPA. Additionally, before a patient is given tPA, hemorrhagic stroke must be ruled out (to prevent excessive, and likely lethal, bleeding) using neuroimaging scans. Due to these limitations, only about 1-3% of acute ischemic stroke patients are estimated to actually receive tPA [61]. Other than tPA, the only agent that has been shown to confer some benefit to patients is aspirin, with less than 1% of patients benefiting measurably [62]. Therefore, more effective and more widely applicable treatments for this condition must be found.

Recently, research has been done to develop neuroprotective therapies to treat ischemic stroke. Since the molecular pathways which are affected during stroke and which lead to cell death have been studied, several key cellular components have been identified as possible therapeutic targets. For instance, as described earlier, excessive

activation of glutamate receptors, intracellular Ca^{2+} accumulation, and initiation of the ER UPR pathways leading to apoptosis are key factors in neuronal cell damage resulting from ischemic stroke. By interrupting one or more of these signaling cascades, the affected neurons may be able to survive. For this reason, several possible neuroprotective agents have recently been studied. These include the selective estrogen receptor modulator raloxifene, which was shown to reduce the glutamate-induced increase in intracellular calcium in rat cortical neurons [63], as well as schizandrin, which was shown to protect cortical neurons from glutamate-induced excitotoxicity, prevent intracellular calcium influx, maintain membrane integrity, and attenuate pro-apoptotic protein synthesis [64]. In addition, the granulocyte colony-stimulating factor (G-CSF), S-methyl-N,N-diethylthiolcarbamate sulfoxide (DETC-MeSO), and taurine have also been studied for their neuroprotective effects [65-69].

G-CSF is currently approved for use as a treatment of neutropenia (low neutrophil level); it is also used in bone marrow reconstitution and stem cell mobilization [70]. As a 20-kDa member of the cytokine family of growth factors, G-CSF works primarily by stimulating cell proliferation, differentiation, and maturation by binding to specific G-CSF receptors [71]. The G-CSF protein has already been shown to be a neuroprotective agent against stroke, Parkinson's disease, and Alzheimer's disease [72-75], but it has not yet been approved for these uses. Interestingly, there is evidence that G-CSF strongly improves post-stroke recovery of the sensorimotor and cognitive functions describe above, perhaps by its ability to enhance neurogenesis (new neuron formation) and angiogenesis (new blood vessel formation) in the infarcted brain [76-78].

DETC-MeSO is an active metabolite of disulfiram, a drug used to treat alcoholism for over 60 years [79]. In fact, disulfiram undergoes bioactivation *in vivo* to give DETC-MeSO, which is actually the active agent to give the anti-alcoholic effect [80]. DETC-MeSO has been shown in mice to act as an antagonist of brain glutamate receptors [81]. Specifically, it is a potent and selective carbamoylating agent of the sulfhydryl groups in glutamate receptors (NMDA and other receptors), and it has been shown to partially inhibit glutamate binding to synaptic membrane preparations from mice [82].

Taurine is a sulfur-containing, free amino acid that is present in high concentrations in several organs in most mammals, including the brain [83]. Taurine mediates many physiological functions including regulation of Ca^{2+} -dependent processes, osmoregulation, membrane stabilization, neurotransmission, and neuroprotection [84-88]. It has also been shown to help reduce ER stress in C2C12 (mouse myocytes) and 3T3L1 (mouse adipocytes) [89]. Moreover, it has been shown to prevent many harmful metabolic events caused by ischemia, as well as to attenuate Ca^{2+} influx, and thereby act as a neuroprotective agent [90-93].

Still, it remains that only one very narrowly applicable treatment for acute ischemic stroke exists, making new, more effective and applicable treatments necessary. Since the biological effects that cause damage to neurons during an ischemic stroke include glutamate excitotoxicity, intracellular calcium overload, and eventually inhibition of pro-survival proteins via the UPR in the ER, a reasonable strategy to develop more

effective treatments for ischemic stroke is to investigate calcium antagonists, glutamate antagonists, and other potential neuroprotective agents.

1.3. The current stroke-related research model

Stroke, as mentioned above, is the 3rd leading cause of death in the U.S.; however, in contrast to the top 2 causes of death (heart disease and cancer), stroke is an extremely under-treated disease. Existing therapies must be improved, and a vigorous search for new therapies should be undertaken. In light of the great need for better treatments for stroke and in light of the potential for discovering certain conopeptides capable of treating stroke via interaction with neuronal ion channels or GPCRs to yield neuroprotective effects [22], the goal of the current work was to isolate and characterize peptides from the dissected venom of the cone snail *Conus brunneus*, and to test them for potential neuroprotective activity in a stroke-related model of induced glutamate excitotoxicity (leading to cell death) in primary rat neuronal cells and in PC12 pheochromocytoma cells.

2. MATERIALS AND METHODS

2.1. Materials

Several materials were necessary to carry out all of the biological testing. These included F-12K media, trypsin-EDTA solution, heat-inactivated horse serum (HS), and rat pheochromocytoma PC12 cell line, which were purchased from ATCC (Manassas, VA, USA). Meanwhile, basal medium eagle (BME), heat-inactivated fetal bovine serum (FBS), poly-D-lysine (PDL), L-glutamine, D-glucose, taurine (Tau), penicillin-streptomycin solution, calpain, mammalian protease inhibitor cocktail, and other chemicals were purchased from Sigma-Aldrich (St. Louis, MO, USA). Neurobasal medium and B27 supplement were purchased from Invitrogen (Carlsbad, CA, USA). Rabbit anti-Bcl-2 and anti-caspase-12, as well as the secondary antibodies were purchased from Santa Cruz Biotechnology (Santa Cruz, CA, USA). Similarly, mouse anti-GAPDH and rabbit anti-Akt were purchased from Cell Signaling Technology (Boston, MA, USA). The Cell Titer-Glo® Luminescent Cell Viability Assay (ATP Assay) kit was purchased from Promega (Madison, WI, USA). Radio-Immunoprecipitation Assay (RIPA) buffer, phosphatase inhibitor cocktail, and ECL detection reagents were purchased from ThermoScientific (Rockford, IL, USA). Pregnant Sprague-Dawley rats were purchased from Harlan (Indianapolis, IN, USA) and were housed in the animal care facility at Florida Atlantic University. The rat care and use procedures were approved, in accordance with the National Institutes of Health

Guidelines for the Care and Use of Laboratory Animals, by the Institutional Animal Care and Use Committee of Florida Atlantic University.

2.2. Conopeptide isolation and characterization

Before isolation and subsequent characterization could be done, the venom of the cone snail *C. brunneus* had to be collected and prepared for use. The venom machinery (venom duct, venom bulb, and radular sac) was dissected from the snails on December 27, 2011, and they were stored in 0.1% trifluoroacetic acid (TFA) in H₂O in a -80°C freezer.

Fifteen venom ducts were later thawed, homogenized, and the venom extracted from them. This was done using a basic homogenizer with a stainless steel probe for 2 minutes, followed by centrifuging at 4°C for 20 minutes at 10,000 rpm. A second homogenization using 7.5 mL 0.1% TFA was done on the remaining pellet after the supernatant had been removed into a clean 50-mL tube. Centrifugation was carried out again at the same conditions. A third round of homogenization and centrifugation was done, and all 3 supernatants were combined in a 50-mL tube. The supernatants were frozen at -80°C overnight and later lyophilized. The total dry weight of the crude venom was obtained.

2.2.1. High-performance liquid chromatography (HPLC)

2.2.1.1. Size-exclusion HPLC

Several size-exclusion HPLC runs were done. The following general protocol was followed in each case. To prepare the *C. brunneus* sample, approximately 50 mg of dry crude venom was dissolved in exactly 5.0 mL 0.1 M NH₄CO₃ in a 50-mL tube with

vortexing. The sample was then centrifuged at 4°C for 8 minutes at 10,000 rpm. The supernatant, and if necessary, enough additional NH_4CO_3 to equal 5.0 mL was used in the separation. The pellet was kept and stored at -80°C. An isocratic separation of the 5-mL crude venom extract solution was done using 0.1 M NH_4CO_3 with a flow rate of 1.5 mL/min over 300 minutes, monitoring the absorption at $\lambda = 220$ nm and $\lambda = 280$ nm. Fractions corresponding to each absorption peak in the chromatogram were collected, frozen overnight at -80°C, lyophilized, weighed, and stored for further separation at -80°C.

2.2.1.2. Reverse-phase semi-preparative HPLC

Several semi-prep HPLC runs were done. The following general protocol was followed in each case. To prepare a sample for semi-prep separation, a fraction from a previous size-exclusion separation was used. The 50-mL tube containing the desired fraction (lyophilized) was obtained from the -80°C freezer. The sample was dissolved in 1000 μL 0.1% TFA. The tube was vortexed briefly to dissolve. The sample was centrifuged at 4°C to spin down any remaining solids. The supernatant, and if necessary, enough additional 0.1% TFA to reach 1000 μL was used in the separation. A gradient method was used, going from 100% Solution A (0.1% TFA) to 100% Solution B (60% ACN in 0.1% TFA) over 100 minutes with a flow rate of 3.5 mL/min. The absorbance at $\lambda = 220$ nm and $\lambda = 280$ nm was monitored. Fractions were collected in 5-mL tubes, corresponding to each absorption peak in the chromatogram. They were dried overnight using a speed-vac and stored at 4°C. The collection times were also recorded. (All solutions were de-gased and the column cleaned and purged prior to use.)

2.2.1.3. Reverse-phase analytical HPLC

Several analytical HPLC runs were done. The following general protocol was followed in each case. To prepare a sample for analytical separation, a fraction from a previous semi-prep separation was used. The 5-mL tube containing the desired fraction was obtained from the 4°C refrigerator. The sample was dissolved in 500 µL 0.1% TFA in a 1.5-mL Eppendorf tube. The tube was vortexed briefly to dissolve. A micro-centrifuge was used for a few seconds to spin down any remaining solids. The supernatant, and if necessary, enough additional 0.1% TFA to reach 500 µL was used in the separation. A gradient method was used, going from 100% Solution A (0.1% TFA) to 100% Solution B (60% ACN in 0.1% TFA) over 100 minutes with a flow rate of 1.0 mL/min. The absorbance at $\lambda = 220$ nm (R: 0.5, 1, 3) and $\lambda = 280$ nm (R: 1) was monitored. Fractions were collected in 1.5-mL Eppendorf tubes, corresponding to each absorption peak in the chromatogram. They were dried overnight using a speed-vac and stored at 4°C. The collection times were also recorded. (All solutions were de-gased and the column cleaned and purged prior to use.)

2.2.2. Matrix-assisted laser desorption/ionization-mass spectrometry (MALDI-MS)

The MALDI matrix solution that was used was prepared at least one day in advance. First, a small amount (20-25 mg) of raw α -C4HCA (α -cyano-4-hydroxycinnamic acid) was obtained from its brown glass bottle in a -20°C freezer and was placed in a black 1.5-mL Eppendorf tube. To it was added 1.0 mL of 36% MeOH/56% ACN/8% H₂O. The mixture was vortexed for 10-15 seconds and stored at room temperature for later use.

To prepare samples for MALDI-MS, a magnetic insert 192 MALDI plate was cleaned with MeOH and H₂O and dried completely. Once dry, 0.3 µL of MALDI matrix solution (described above) was deposited in each well desired for use and was allowed to dry completely. During this time, the desired peptide fractions were prepared for MALDI analysis. For peptide fractions corresponding to more intense (higher UV-Vis absorption) chromatogram peaks, 100 µL of Solution B (60% ACN in 0.1% TFA) was added to the dry sample, whereas for fractions corresponding to less intense peaks, 40 µL of the same solution was added to the dry sample. Each sample was vortexed for about 5 seconds. Once the MALDI matrix had dried, 0.3 µL of each sample was placed in a separate well, and the samples were allowed to dry completely.

Several MALDI-MS experiments were done. The following general protocol was followed in each case. To carry out the MALDI-MS runs, a Voyager-DE STR (Applied Biosystems) MALDI-TOF was used. Either reflector or linear mode was selected, with reflector mode being more accurate and linear mode being more sensitive. Laser intensity was set at 2400, and shots/spectrum was set at 100, with an initial mass detection range of 800-5000 Da. Each sample was positioned, one at a time, beneath the laser beam, and a joystick was used to direct the laser throughout the course of each run. Several runs for each sample were sometimes necessary. For each sample, the major mass peaks were recorded manually, and images of the mass spectra collected for further analysis.

2.2.3. Nuclear magnetic resonance (NMR) spectroscopy

To prepare peptide fractions for NMR analysis, the sample was dissolved in 37 µL H₂O + 1.5 µL D₂O + 1.5 µL D₂O/TSP. The sample was vortexed, and transferred

to a 1.7-mm glass capillary NMR tube to give a column height of 30-33 mm. Two NMR experiments were done for each sample: 1D ^1H and 2D TOCSY spectra.

2.2.4. Bioinformatics database comparison (Conoserver)

The peptides that were not identified by comparison to data collected on peptides previously characterized in this laboratory were investigated using the web-based conopeptide database Conoserver for data comparison. Searches were carried out based on molecular weight (with a range of ± 10 Da).

2.3. Cell cultures

2.3.1. Primary neuronal cell culture

Several primary neuronal cell cultures were prepared from embryonic rat neuronal cells. The general protocol is outlined here. The primary neuronal cell cultures were prepared as previously described [71]. In brief, a 17-day pregnant Sprague-Dawley rat was sacrificed using isofluorane. The embryos were removed from the womb, and the brains were removed aseptically and placed in 5 mL of Growth Medium Eagle (GME). The GME consisted of 77 mL BME, supplemented with 1 mL 200 mM L-glutamine, 2 mL 26.8 mM D-glucose, and 20 mL 20% heat-inactivated FBS. The cerebral cortices of the brains were isolated and placed in 2 mL of fresh GME. They were passed through a 14-G cannula to disperse the material and give a homogeneous suspension. This mixture was added to a 15-mL tube containing 5 mL GME, and the solution was passed several times more through the 14-G cannula. The neuronal cell suspension was centrifuged at 500 rpm for 5 minutes at room temperature. The supernatant was discarded, and the pellet was re-suspended in 7 mL of GME. The centrifugation and re-suspension was repeated 3

times. To re-suspend the pellet for plating the cells in 6-, 12-, or 24-well plates, the following formula was used to calculate the volume (mL) of GME to add:

$$[(\# \text{ brains} \times 2) - 2] \times 2 / 10$$

Between 1.0-2.0 mL/well of this suspension was used in plating for these sizes of well plates. For 96-well plates, the remaining volume (mL) of re-suspended pellet after plating 6-, 12-, and 24-well plates was measured. One-third of the remaining volume was calculated and that amount of additional GME was added to the suspension. For the 96-well plates, 100 μ L/well of the suspension was used in plating. (All cell culture plates were pre-coated with PDL by incubating at 37°C overnight with 1.5 mL-80 μ L of 0.5 mg/mL PDL, depending on plate size, and then rinsing with H₂O prior to cell plating.). The cell culture plates were incubated in a humidified incubator (37°C, 99% humidity, 5% CO₂) for 30-45 minutes. Finally, the GME was replaced with serum-free Neurobasal Medium (NB) supplemented with 2% (v/v) B27 and 0.25% (v/v) 500 μ M L-glutamine. The cells were maintained in the same incubator for 12-18 days until ready for use in biological assays.

2.3.2. PC12 cell culture

PC12 cells were maintained at 37°C/99% humidity/5% CO₂ in F12-K medium supplemented with 10% (v/v) FBS (for easier growth), 15% (v/v) heat-inactivated HS, and 1% (v/v) penicillin-streptomycin solution. All experiments were performed on undifferentiated cells plated in 96-well plates at a density of $\sim 5 \times 10^4$ cells/mL for the ATP assay and in 60-mm Petri dishes at $\sim 3 \times 10^5$ cells/well for the Western Blot analysis 24 hours prior to experiments. (The well plates and Petri dishes were pre-coated with PDL as described above.)

2.4. Glutamate excitotoxicity stroke-related model

To carry out experiments on the glutamate excitotoxicity-induced stroke-related model in primary neuronal cells and PC12 cells, the cells were pre-incubated with the positive control taurine and/or with the desired peptide test fraction for a certain amount of time. The cells were then treated with a specific amount of glutamate for a given amount of time. Cell survival was tested using the ATP assay and Western Blot analysis. Appropriate controls were also tested. (Primary neuronal cell cultures were used between 12-18 days *in vitro*.)

2.4.1. Cell viability – ATP assay

The Cell Titer-Glo® Luminescent Cell Viability Assay (Promega) was carried out according to the literature provided with the kit. The prepared cell cultures (primary embryonic rat neurons or PC12 cells) in 96-, 24-, 12-, or 6-well clear poly-D-lysine-coated culture plates were used. For the 96-well plates, the recommended 100 µL of cell culture was used, and for the larger well-plates, a proportionately greater volume of cell culture was used. In the assays, either simultaneous treatment (taurine + glutamate, or peptide fraction + glutamate) or pre-treatment (taurine or peptide fraction before glutamate) was done. Simultaneous treatment was done in many of the earlier assays, while pre-treatment was done in the later assays. After the addition of a range of concentrations of positive control compound (taurine) or peptide fraction (A-F) to each experimental well, the plates were incubated (37°C, 99% humidity, 5% CO₂) for varying periods of time, followed by the addition of certain concentrations of glutamate. Glutamate (negative) control wells were also treated at this time, followed by a period of

incubation. After this incubation time, the plates were removed from the incubator. Once equilibrated to room temperature, a volume of Cell Titer-Glo® Reagent equal to the volume of cell culture medium present in each well was added. The plates were then placed on an orbital shaker for 2 minutes to induce cell lysis, followed by a 10-minute incubation at room temperature for luminescent signal (from luciferase reaction) stabilization. Finally, the contents of the wells were transferred to an opaque (white) 96-well plate and the luminescence intensity was recorded using an M3 SpectaMax (Molecular Devices).

Control wells containing medium only (without cells) were always prepared to obtain a value for background luminescence. The ATP content from treated wells was expressed as a percentage of the ATP content from untreated control wells (100%). Peptide test fraction concentrations were determined on a ThermoScientific NanoDrop 2000/2000c using the A₂₀₅ Custom Method for Protein and Peptide Quantification, which monitors the absorption of the peptide bond, with sensitivity up to 0.001 µg/µL. (Separate experiments in which control wells for each of the treatment compounds and peptide fractions (with and without cells) were also carried out.)

2.4.2. Protein expression – Western blot analysis

For Western Blot analysis, primary neuronal or PC12 cell cultures were pre-treated with peptide fraction, followed by exposure to glutamate. Then, the cells were lysed in RIPA buffer (25 mM Tris-HCl, 150 mM NaCl, 1% NP-40, 1% sodium deoxycholate, 0.1% SDS; pH 7.6) containing 1% (v/v) mammalian protease inhibitor cocktail and 1% (v/v) phosphatase inhibitor cocktail to protect proteins from degrading.

The proteins in the cell lysates were separated via SDS-PAGE and transferred to a nitrocellulose membrane. The membrane was blocked in blocking buffer (20 mM Tris-HCl, 150 mM NaCl, 0.1% Tween-20, 5% milk; pH 7.6) for 2 hours at room temperature. After blocking, the desired primary antibody was added and left at room temperature to incubate overnight. This was followed by 2 hours of incubation at room temperature with the corresponding HRP-conjugated secondary antibody to yield a chemiluminescent signal. Extensive washes with blocking buffer were performed between each step. The protein-immuno complex was visualized using the ECL detection reagents purchased from ThermoScientific.

3. RESULTS AND DISCUSSION

3.1. Conopeptide isolation and characterization

3.1.1. High-performance liquid chromatography (HPLC)

3.1.1.1. Size-exclusion HPLC

The dissected venom from *C. brunneus* was separated first using size-exclusion HPLC, as described above. The larger proteins and peptides eluted at the beginning of the separation, followed by smaller peptides. A representative size-exclusion chromatogram is shown below in Figures 9 ($\lambda = 220$ nm) and 10 ($\lambda = 280$ nm). The 220-nm wavelength was chosen to monitor the absorbance of the peptide bond, while the 280-nm wavelength was chosen to monitor the absorbance of tyrosine and tryptophan amino acid residues. Three size-exclusion HPLC runs were performed, and each time, the fraction corresponding to the major peak observed in the $\lambda = 280$ nm chromatogram was selected for further separation via semi-prep HPLC. This was done since interesting and bioactive conopeptides have previously been isolated from the major absorption peak in the $\lambda = 280$ nm chromatogram. A list of fractions collected during the first size-exclusion HPLC run is shown in Table 1 below. It is also representative of all 3 of the size-exclusion runs (as are the chromatograms below), which yielded very similar elution times and peak absorbances.

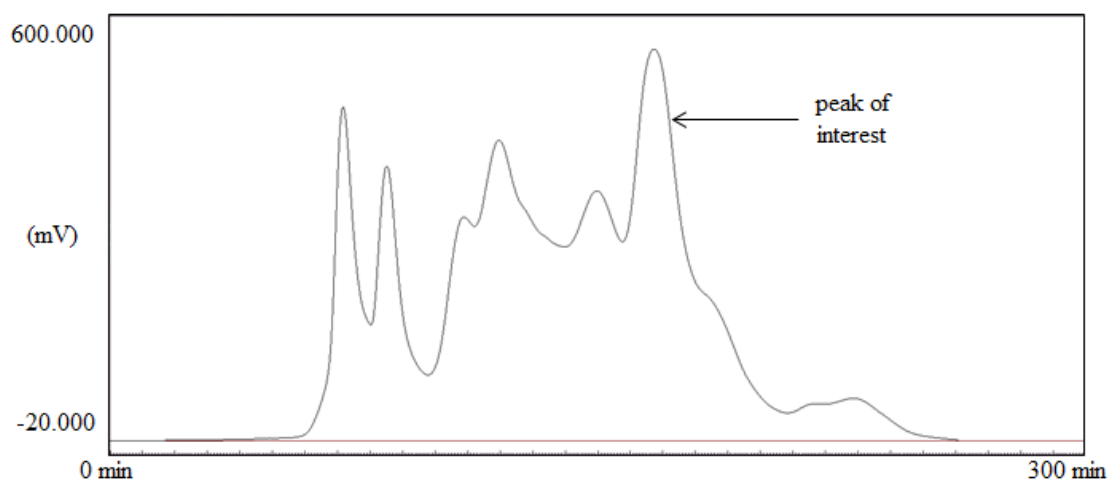


Figure 9. Size-exclusion HPLC chromatogram of *C. brunneus* crude venom extract (absorbance at $\lambda = 220$ nm).

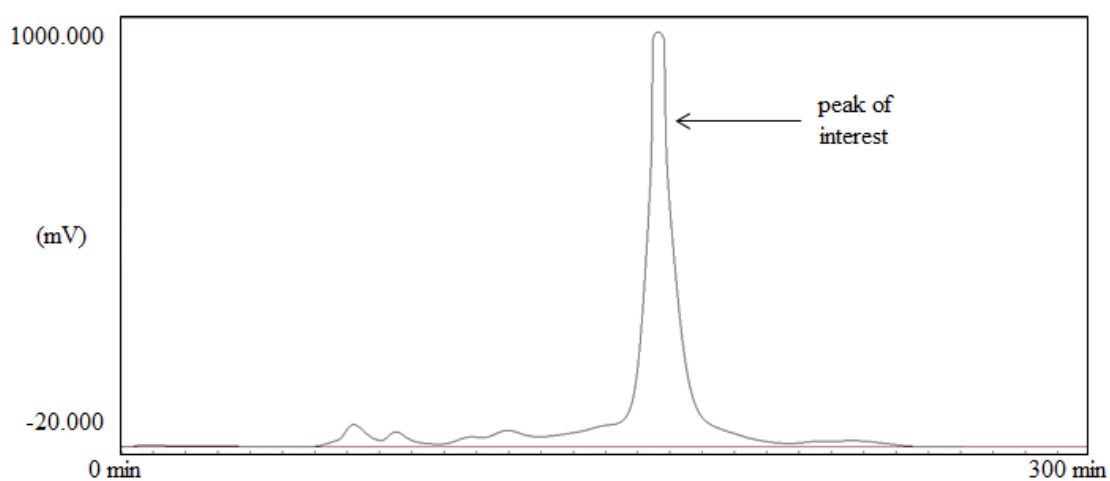


Figure 10. Size-exclusion HPLC chromatogram of *C. brunneus* crude venom extract (absorbance at $\lambda = 280$ nm).

Table 1. Peak table for *C. brunneus* crude venom size-exclusion HPLC separation.

Fraction	Start Time (minutes)	End Time (minutes)
1	50.15	78.09
2	78.10	90.99
3	91.00	101.74
4	101.75	112.99
5	113.00	134.69
6	134.70	159.44
7*	159.45	185.84
8	185.85	206.34
9	206.35	233.49
10	233.50	261.08

*Fraction 7 was the major peak in the $\lambda = 280$ nm absorbance chromatogram.

3.1.1.2. Reverse-phase semi-preparative HPLC

After size-exclusion HPLC, the fraction of crude venom containing the major $\lambda = 280$ nm peak was further separated using semi-prep HPLC, as described above. The more polar peptides eluted at the beginning of the separation, followed by less polar peptides. A representative semi-prep HPLC chromatogram is shown below in Figures 11 and 12 (absorbance at $\lambda = 220$ nm) and 13 and 14 (absorbance at $\lambda = 280$ nm). Several semi-prep runs were performed, and each time, the fractions were analyzed using MALDI-MS (results shown below) before combining fractions. The fraction combining was based on elution time and molecular weight. The combined peptide fractions were used in the ATP assays and Western blot analysis (results shown below). A list of the relevant semi-prep fractions is shown in Table 2 below.

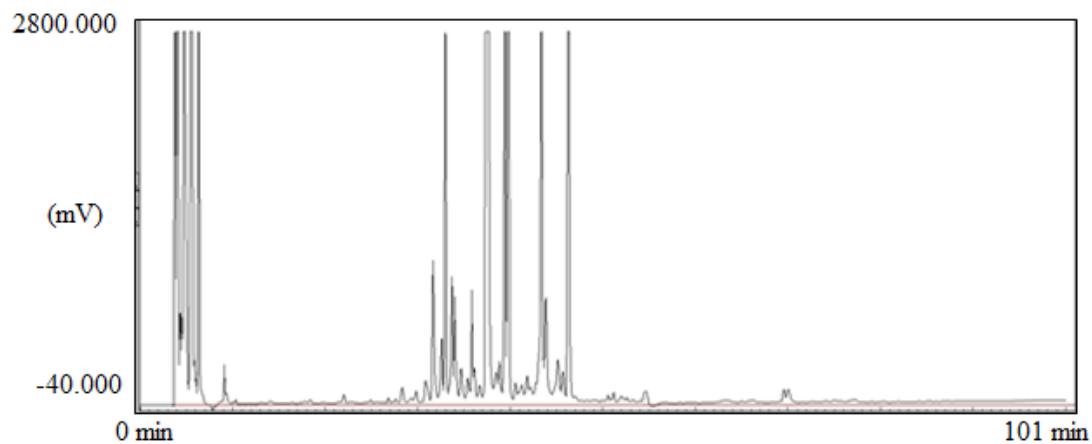


Figure 11. Semi-prep HPLC chromatogram of *C. brunneus* fraction from size-exclusion (absorbance at $\lambda = 220$ nm).

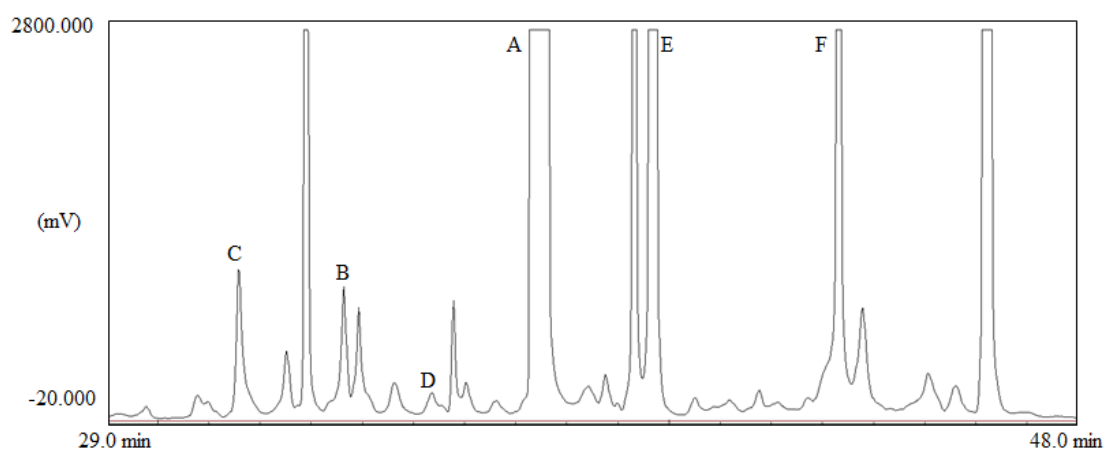


Figure 12. Semi-prep HPLC chromatogram of *C. brunneus* fraction from size-exclusion (absorbance at $\lambda = 220$ nm), zoomed-in.

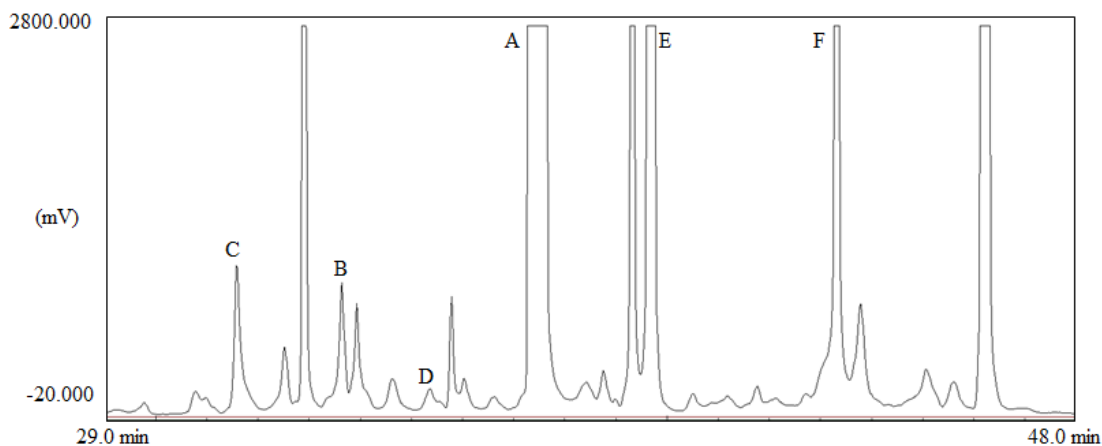


Figure 13. Semi-prep HPLC chromatogram of *C. brunneus* fraction from size-exclusion chromatography (absorbance at $\lambda = 280$ nm).

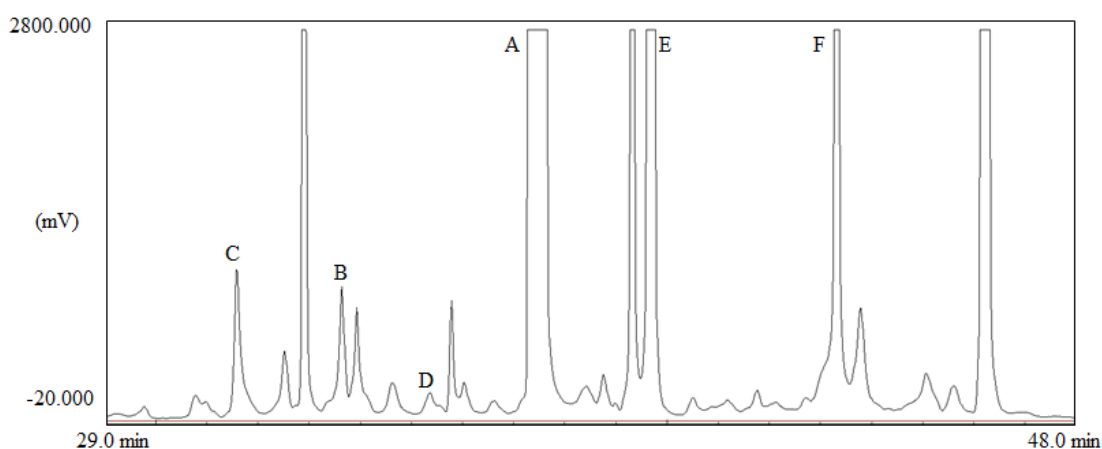


Figure 14. Semi-prep HPLC chromatogram of *C. brunneus* fraction from size-exclusion chromatography (absorbance at $\lambda = 280$ nm), zoomed-in.

Table 2. Relevant peak table for semi-prep HPLC separation of the major $\lambda = 280$ nm absorbance peak from the size-exclusion fraction of *C. brunneus*.

Peptide Fraction	Start Time (minutes)	End Time (minutes)
A	37.07	38.16
B	33.29	33.91
C	31.41	32.17
D	35.15	35.79
E	39.60	40.46
F	42.58	43.65

3.1.1.3. Reverse-phase analytical HPLC

Several analytical HPLC runs were carried out on peptide fraction A, as described above, to better purify it for further biological and analytical testing. A representative analytical HPLC chromatogram is shown below in Figures 15, 16, 17 ($\lambda = 220$ nm), and 18 ($\lambda = 280$ nm). The fractions from these analytical runs were analyzed using MALDI-MS before combining fractions, based on elution time and molecular weight. Only fractions containing apparently pure peptide A (based on molecular weight) were combined and kept for further testing.

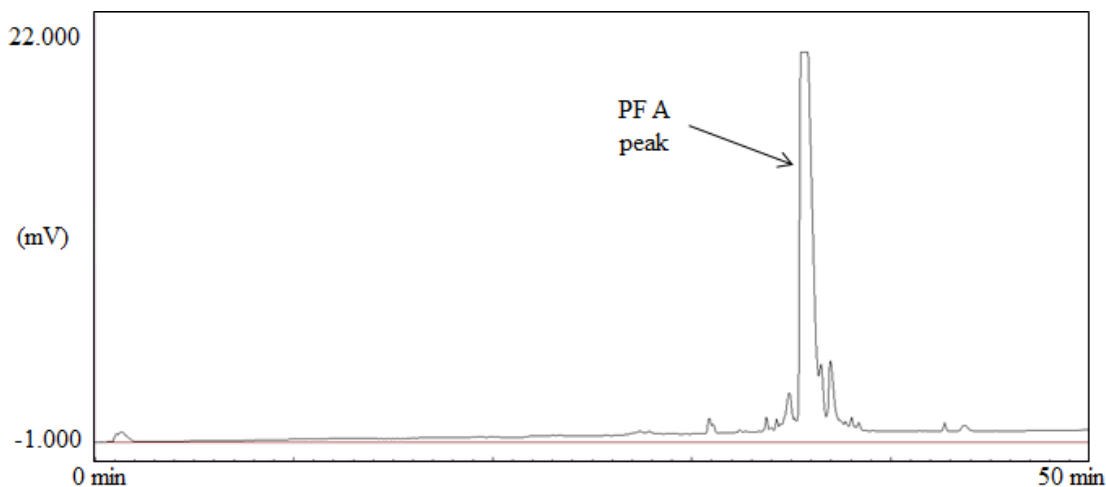


Figure 15. Analytical HPLC chromatogram of *C. brunneus* peptide fraction A
(absorbance at $\lambda = 220$ nm; R: 0.5).

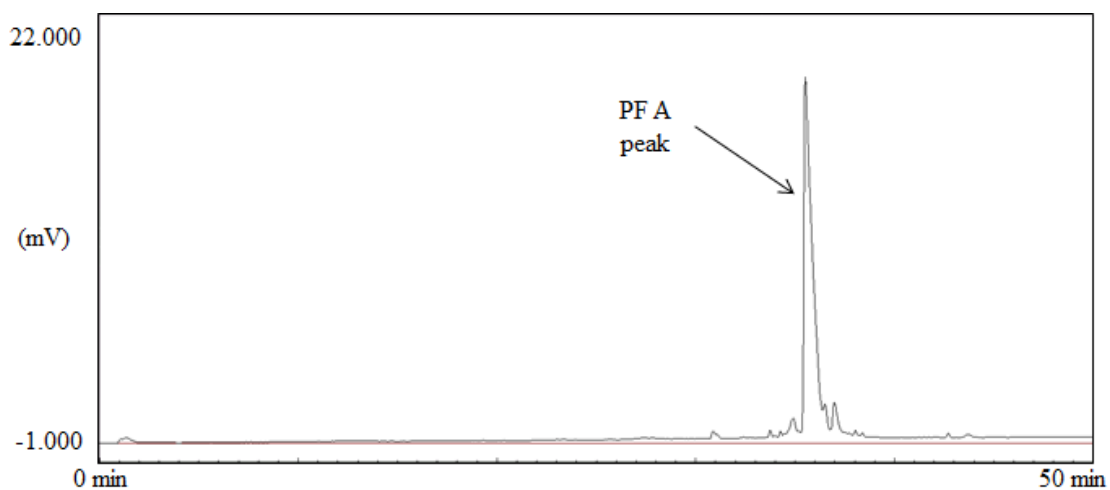


Figure 16. Analytical HPLC chromatogram of *C. brunneus* peptide fraction A
(absorbance at $\lambda = 220$ nm; R: 1.0).

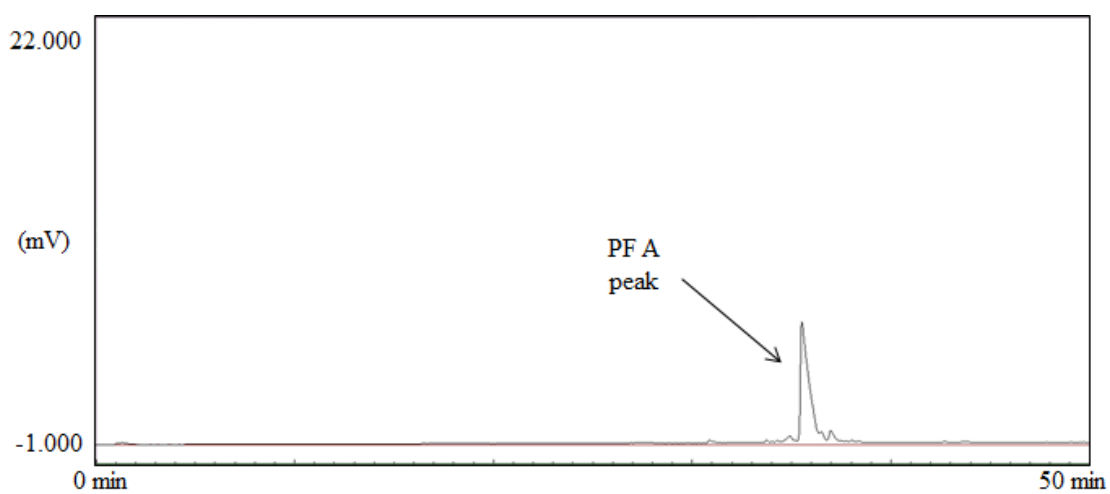


Figure 17. Analytical HPLC chromatogram of *C. brunneus* peptide fraction A
(absorbance at $\lambda = 220$ nm; R: 3.0).

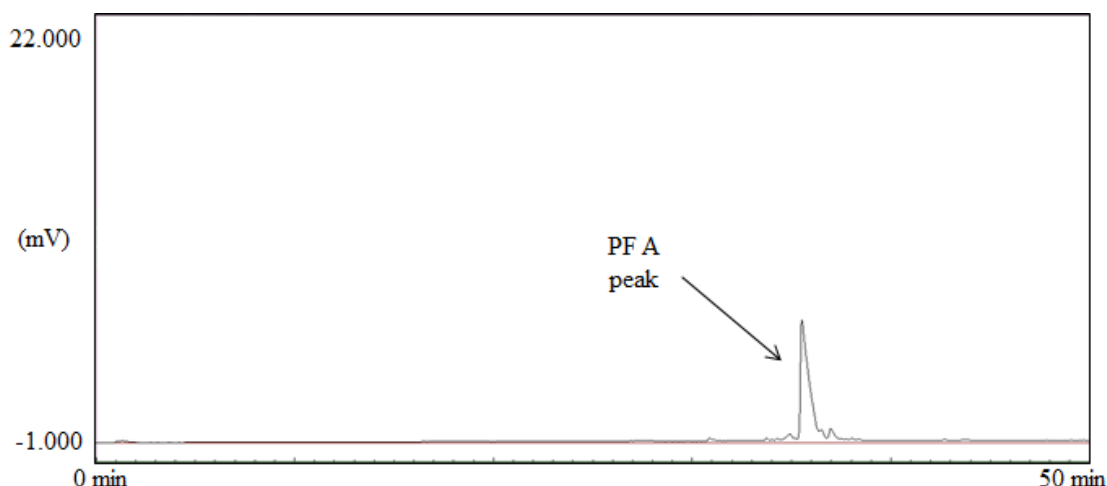


Figure 18. Analytical HPLC chromatogram of *C. brunneus* peptide fraction A
(absorbance at $\lambda = 280$ nm).

3.1.2. Matrix-assisted laser desorption/ionization-mass spec (MALDI-MS)

MALDI-TOF MS (Voyager-DE STR, Applied Biosystems) spectra were obtained for each peptide fraction from *C. brunneus* to aid in fraction combining and peptide identification, with representative spectra in Figures 19-24 for peptide fractions A-F. Based on the MALDI spectra collected, the probable identities of 3 of the peptides isolated from *C. brunneus* were determined, based on the data from previously characterized peptides in this laboratory. As seen in Figure 19 below, a mass peak of 2533 Da was observed, which suggested that this peptide was bru9a (previously, 2534 Da). Similarly, Figure 23 below shows a mass peak of 2357 Da, and this suggested the peptide may be an α -conotoxin (previously, 2360 Da). And, finally, Figure 24 below shows a mass peak of 2127 Da, which matched exactly the molecular weight of bru3a. The identities of the other peptides could not be determined from MALDI data.

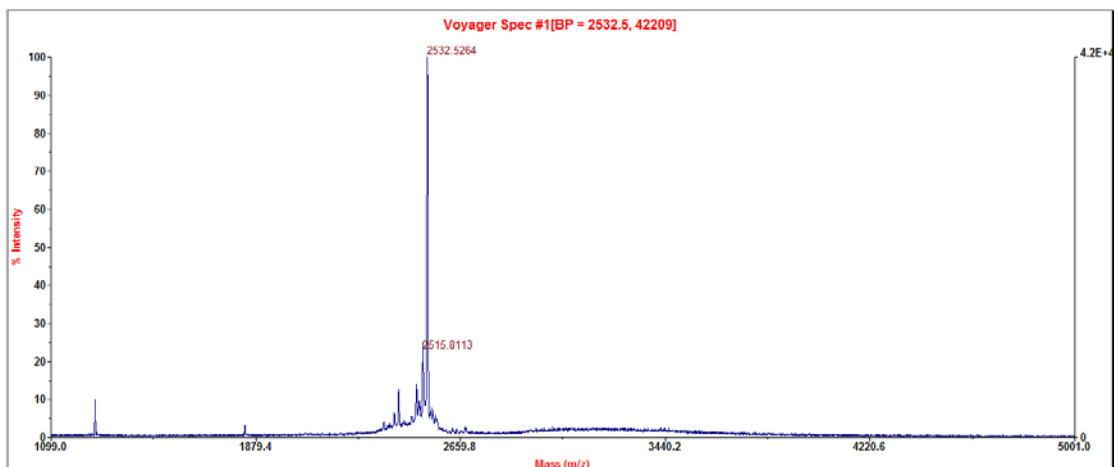


Figure 19. Representative MALDI-MS spectrum for peptide fraction A from *C. brunneus*. A mass peak of 2533 Da was observed.

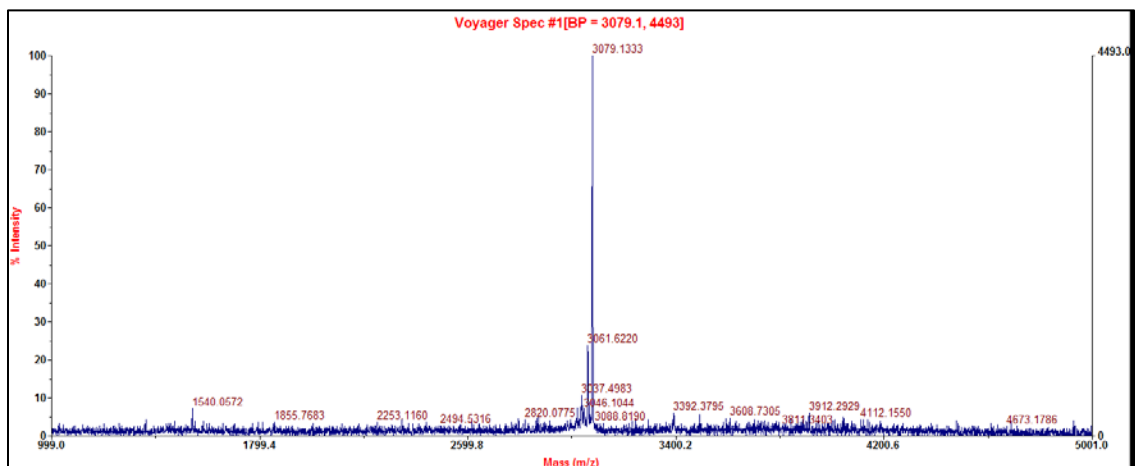


Figure 20. Representative MALDI-MS spectrum for peptide fraction B from *C. brunneus*. A mass peak of 3079 Da was observed.

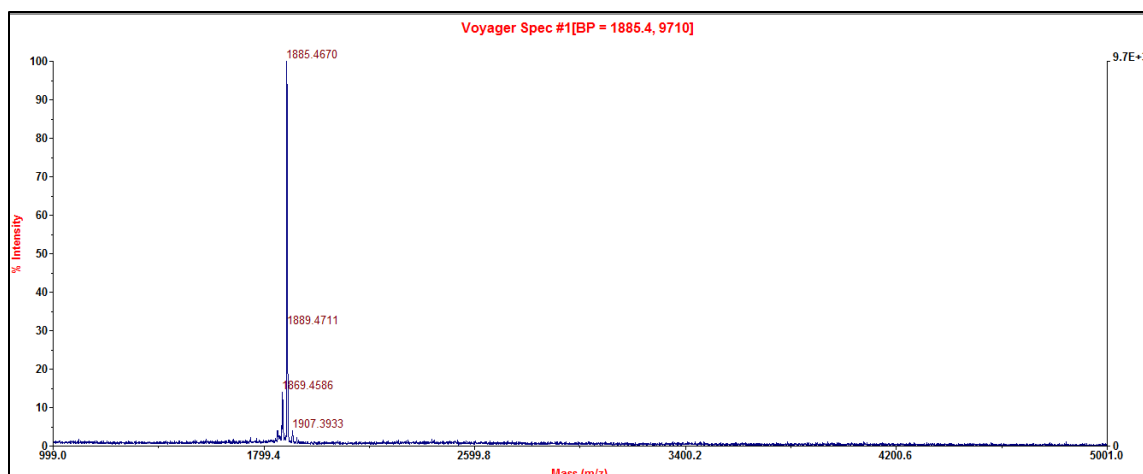


Figure 21. Representative MALDI-MS spectrum for peptide fraction C from *C. brunneus*. A mass peak of 1885 Da was observed.

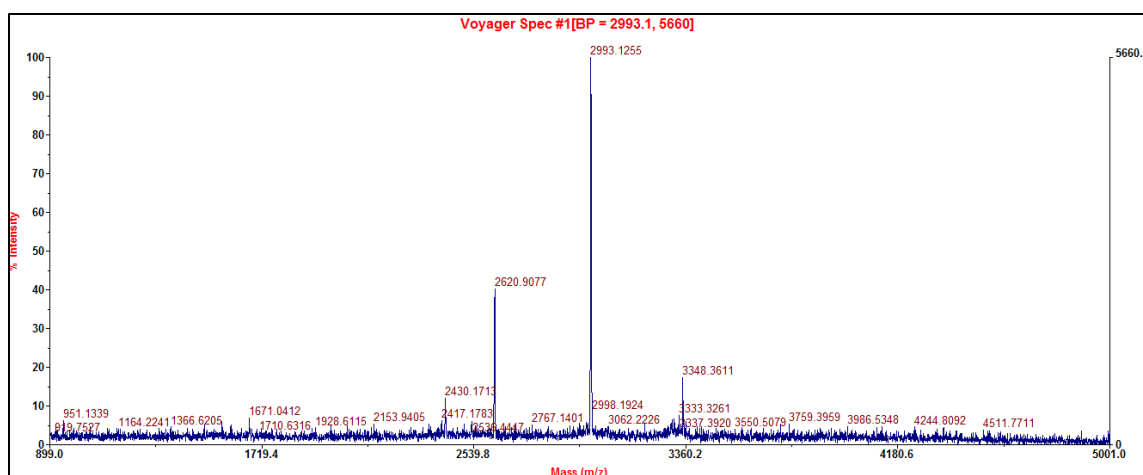


Figure 22. Representative MALDI-MS spectrum for peptide fraction D from *C. brunneus*. Two mass peaks of 2993 and 2621 Da were observed.

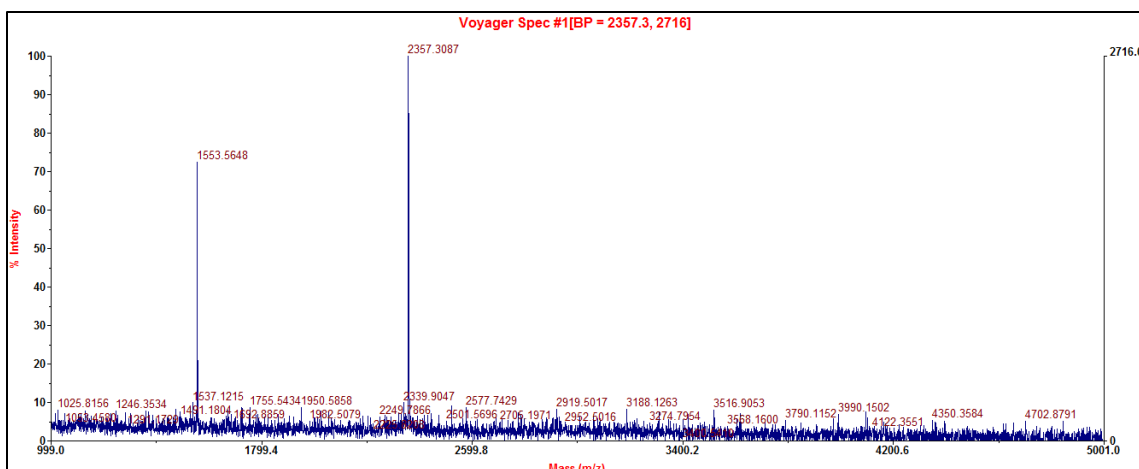


Figure 23. Representative MALDI-MS spectrum for peptide fraction E from *C. brunneus*. Two mass peaks of 2357 and 1554 Da were observed.

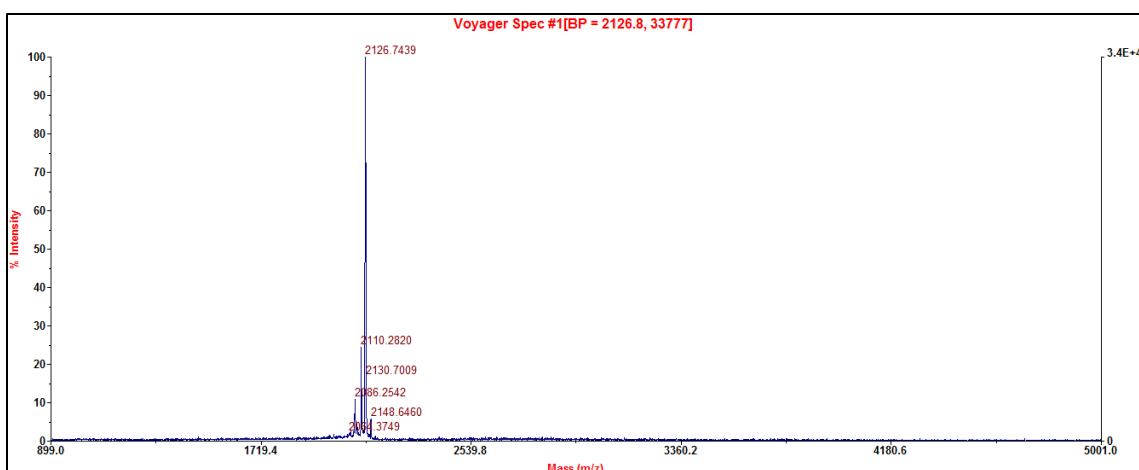


Figure 24. Representative MALDI-MS spectrum for peptide fraction F from *C. brunneus*. A mass peak of 2127 Da was observed.

3.1.3. Nuclear magnetic resonance (NMR) spectroscopy

NMR spectra were obtained as described above for peptide fractions A, C, and F, using a Varian Inova 500 MHz spectrometer. The spectra (^1H and TOCSY) for each of these are shown below in Figures 25-30. A list of chemical shift correlations for peptide fraction A is shown below in Table 3, along with a list of chemical shift correlations for

the previously characterized (in this laboratory) peptide bru9a (described above) from *C. brunneus* shown in Table 4. Comparison of the two tables clearly shows that the peptide in peptide fraction A (2533 Da) is most likely bru9a. The NMR data for the other two peptide fractions are shown, but were not yet able to be interpreted. However, based on molecular weight, the spectra shown in Figures 29 and 30 most likely correspond to the sequence of the bru3a peptide, previously characterized in this laboratory. Clear NMR spectra for the peptide fractions B, D, and E were not obtained as they were either mixtures of peptides (D and E) or had an insufficient concentration of peptide (B).

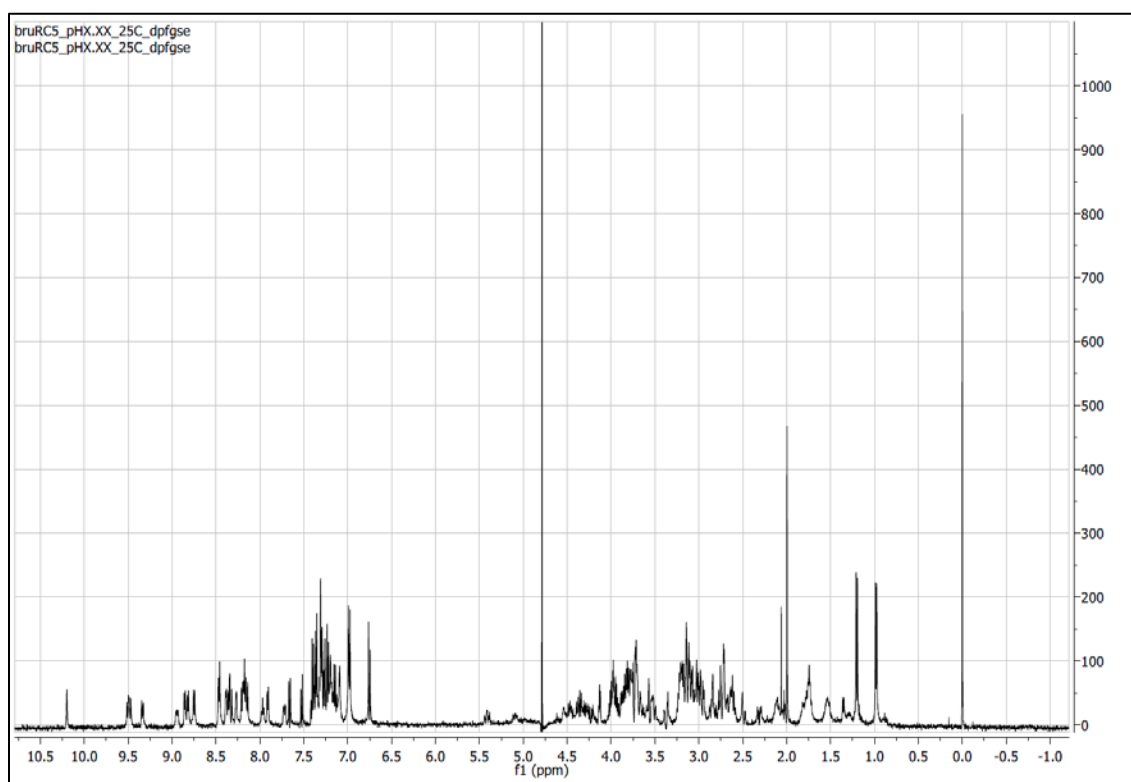


Figure 25. ¹H NMR spectrum of peptide fraction A (2533 Da) from *C. brunneus*.

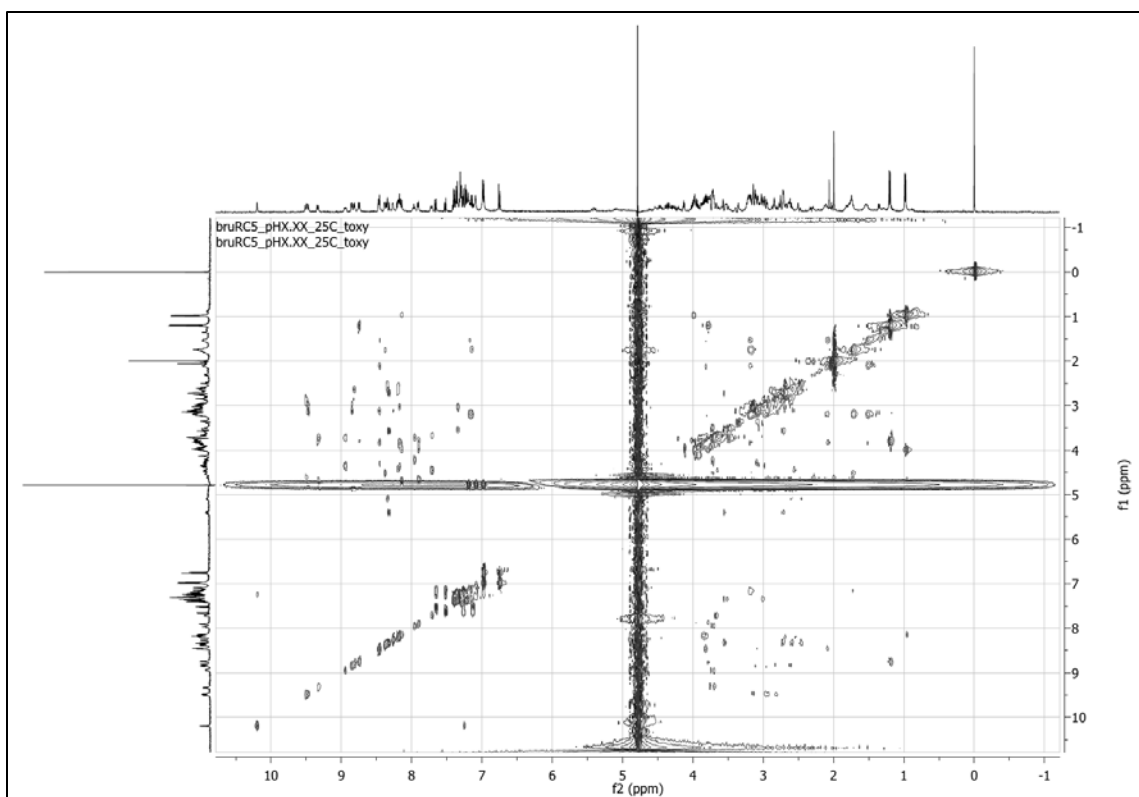


Figure 26. TOCSY NMR spectrum of peptide fraction A (2533 Da) from *C. brunneus*.

Table 3. ^1H NMR chemical shifts of peptide fraction A (2533 Da) from *C. brunneus*.

Amino Acid	HN (ppm)	H α (ppm)	H β (ppm)	Others
Ser1		4.12	3.91, 3.97	
Cys2	8.78	4.86	2.63, 2.84	
Gly3	7.35	3.02, 3.55		
Gly4	7.95	3.72, 4.23		
Ser5	7.90	4.63	3.79, 3.99	
Cys6	8.45	4.28	3.07, 3.14	
Phe7	8.17	4.40	2.96, 3.05	H δ 7.22
				H ϵ 7.36
				H ζ 7.29
Gly8	8.17	3.80, 3.84		
Gly9	7.72	3.68, 4.46		
Cys10	8.84	4.86	2.64, 2.87	
Trp11	8.33	4.79	3.18, 3.57	H δ 7.25
				H ϵ 1 10.20
				H ϵ 3 7.66
				H ζ 2 7.52
				H ζ 3 7.26
				H η 2 7.13
Hyp12		4.51	2.00, 2.31	H δ 3.49, 3.72
Gly13	8.95	3.72, 4.36		
Cys14	8.32	5.40	2.72, 3.55	
Ser15	9.30	4.66	3.70, 3.76	
Cys16	8.85	4.82	2.95, 3.13	
Tyr17	9.49	4.60	2.81, 2.95	H δ 6.98
				H ϵ 6.75
Ala18	8.75	3.79	1.20	
Arg19	8.46	3.82	2.13	H γ 1.53
				H δ 3.15
				H ϵ 7.17
Thr20	8.14	4.67	3.99	H γ 0.98
Cys21	8.34	5.10	2.47, 2.60	
Phe22	9.48	4.59	2.95, 3.15	H δ 7.31
				H ϵ 7.37
				H ζ 7.26
Arg23	8.39	4.55	1.78	H γ 1.74
				H δ 3.18
				H ϵ 7.17
Arg24	8.18	4.41	2.61, 2.68	

*Hyp: hydroxyproline (O)

Table 4. ¹H NMR chemical shift values of bru9a from *C. brunneus* previously characterized in this laboratory. [13]

Amino Acid	HN (ppm)	H α (ppm)	H β (ppm)	Others
Ser1		4.12	3.92, 3.97	
Cys2	8.79	4.78	2.69, 2.76	
Gly3	7.35	3.01, 3.56		
Gly4	7.97	3.73, 4.23		
Ser5	7.92	4.67	3.83, 3.99	
Cys6	8.44	4.30	3.12, 3.19	
Phe7	8.17	4.35	2.98, 3.07	H δ 7.22
				H ϵ 7.36
				H ζ 7.29
Gly8	8.16	3.82, 3.87		
Gly9	7.75	3.66, 4.47		
Cys10	8.87	4.84	2.65, 2.86,	
Trp11	8.33	4.81	3.12, 3.37	H δ 7.25
				H ϵ 1 10.27
				H ϵ 3 7.66
				H ζ 2 7.52
				H ζ 3 7.26
				H η 2 7.13
Hyp12		4.59	2.01, 2.31	H δ 3.48, 3.72
Gly13	8.98	3.72, 4.37		
Cys14	8.35	5.41	2.72, 3.56	
Ser15	9.37	4.72	3.70, 3.80	
Cys16	8.85	4.87	2.98, 3.15	
Tyr17	9.52	4.61	2.81, 2.95	H δ 6.95
				H ϵ 6.76
Ala18	8.78	3.78	1.20	
Arg19	8.46	3.80	2.15	H γ 1.53
				H δ 3.19
				H ϵ 7.18
Thr20	8.15	4.72	4.00	H γ 0.97
Cys21	8.36	5.10	2.49, 2.63	
Phe22	9.48	4.82	2.99, 3.16	H δ 7.31
				H ϵ 7.37
				H ζ 7.26
Arg23	8.46	4.55	1.81	H γ 1.74
				H δ 3.20
				H ϵ 7.16
Arg24	8.24	4.48	2.64, 2.74	

*Hyp: hydroxyproline (O)

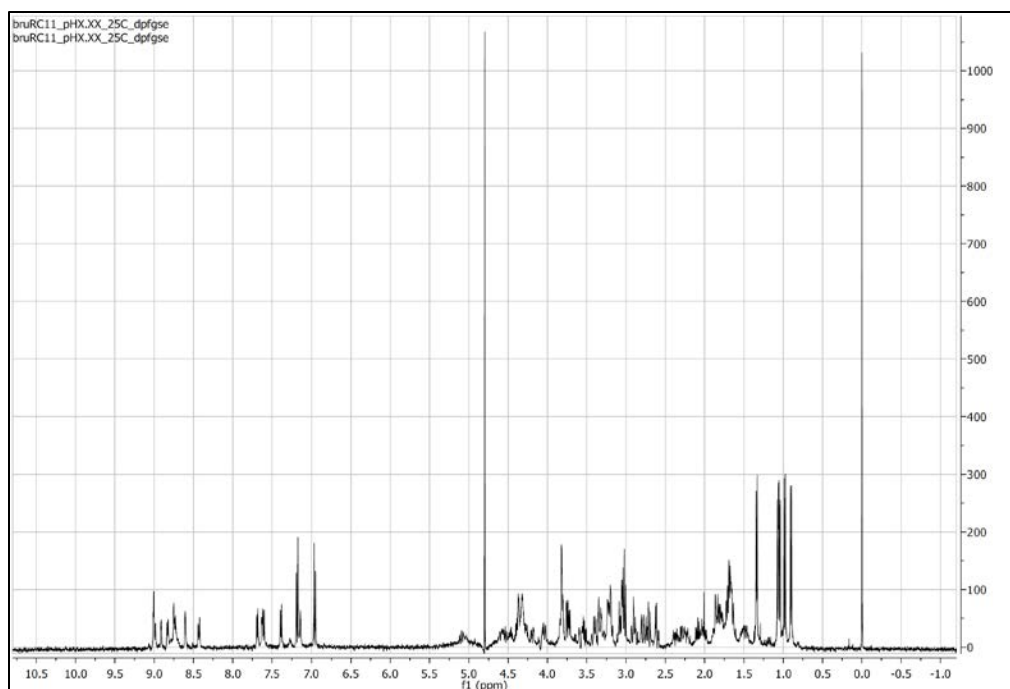


Figure 27. ^1H NMR spectrum of peptide fraction C (1885 Da) from *C. brunneus*.

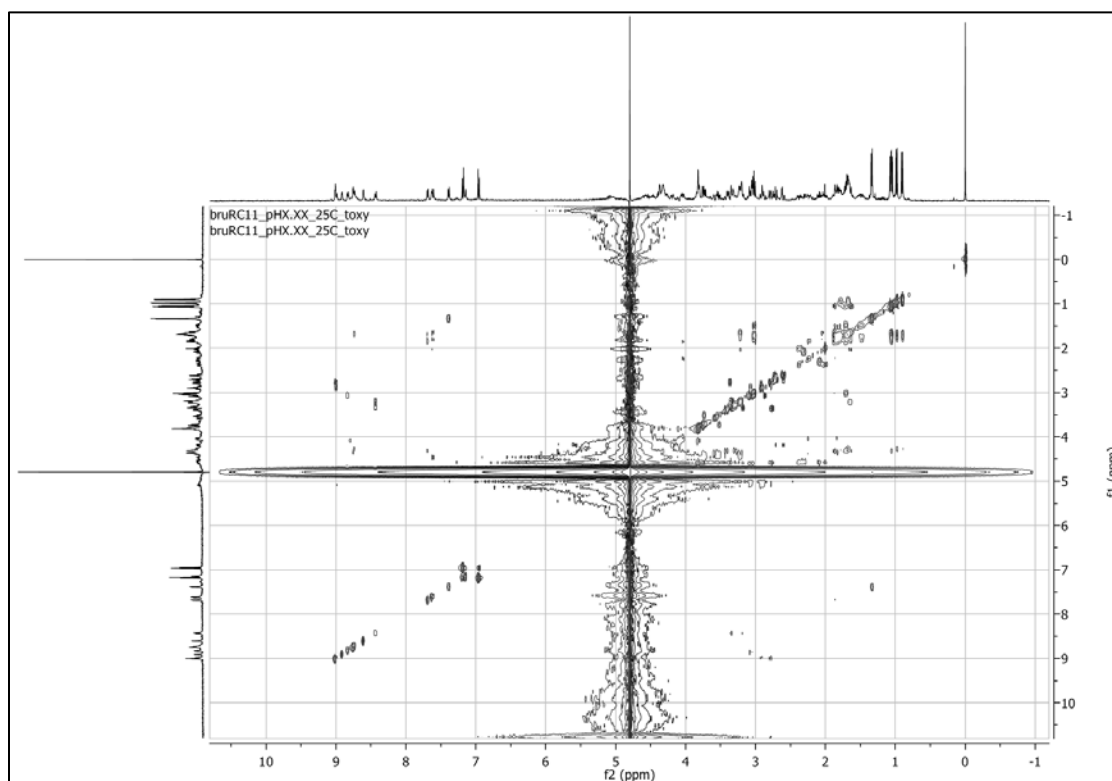


Figure 28. TOCSY NMR spectrum of peptide fraction C (1885 Da) from *C. brunneus*.

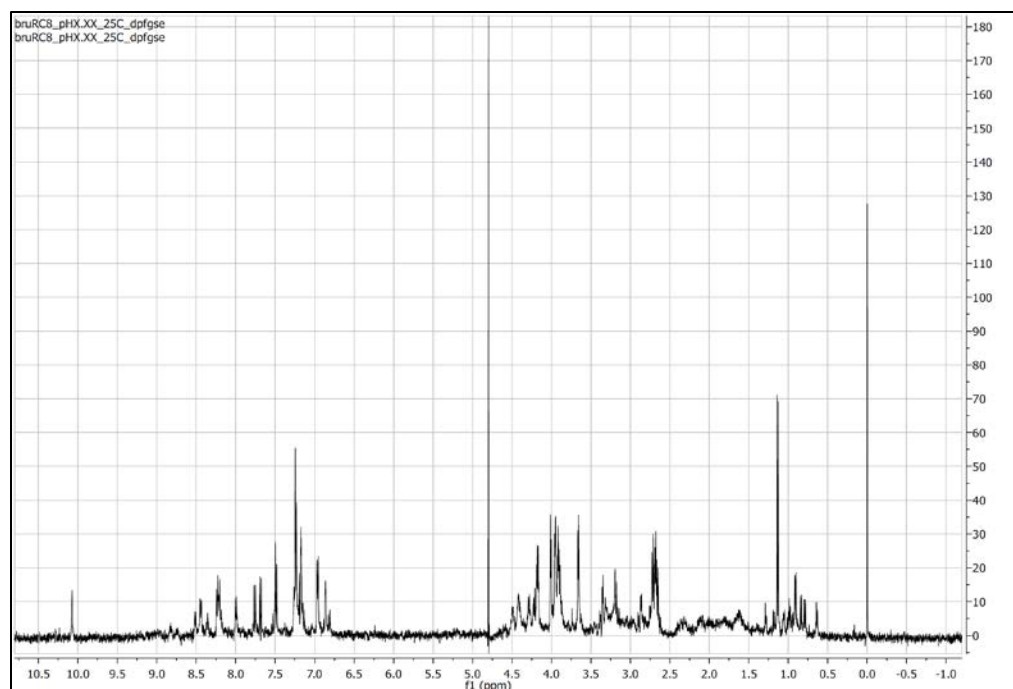


Figure 29. ^1H NMR spectrum of peptide fraction F (2127 Da) from *C. brunneus*.

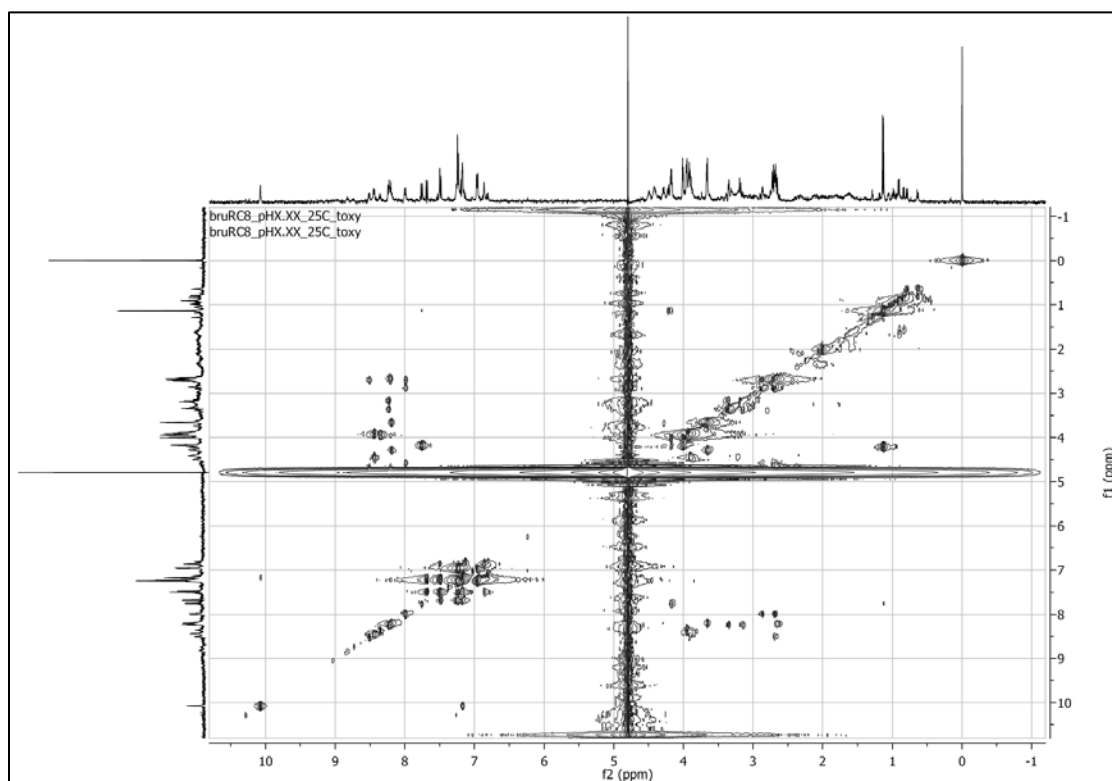


Figure 30. TOCSY NMR spectrum of peptide fraction F (2127 Da) from *C. brunneus*.

A summary of the results of the conopeptide isolation and characterization from *C. brunneus* dissected cone snail venom is shown in Table 5 below.

Table 5. Summary of *C. brunneus* peptide fraction identifying information.

Peptide Fraction	Purity	MW (Da)	Retention Time (min)	Probable Sequence	Probable Identity	Probable Super-family
A	Pure	2533	38	SCGGSCFGGC WOGCSCYAR TCFRD	bru9a	P
B	Pure	3079	35			
C	Pure	1885	32			
D	Impure	2993	36			
		2621	36			
E	Impure	2357	42	TWD γ CCKNP ACRNNHK DKCG	an α -cono-toxin	A
		1554	42			
F	Pure	2127	45	CCRWPRCNV YLCGOCCOQ	bru3a	M

*O: hydroxyproline ($M^+ +6$); γ : γ -carboxyglutamate ($M^+ +44$)

**Purity was assessed based on quality of MALDI-MS spectra and NMR spectra.

3.1.4. Bioinformatics database comparison (Conoserver)

The peptides that were not identified by comparison to peptides previously characterized in this laboratory were investigated using the web-based peptide database Conoserver for data comparison. Based on the search results, several conopeptides were found to be similar in molecular weight. The results for each peptide fraction are listed below in Tables 6-10.

For PF B (3079 Da), 4 conopeptides with similar molecular weights were found in Conoserver and are listed in Table 6 below. All 4 of the peptides found were in the O superfamily, specifically in O1. While 3 of them were isolated from vermivorous cone

snails, 1 was isolated from a molluscivorous snail (*C. marmoreus*). The last two peptides in the table are exactly the same, but were found in two different cone snails.

Table 6. Conoserver search results for conopeptides with similar MW to PF B (3079 Da).

Name	Cone Snail	MW (Da)	Sequence
MaIr193	<i>C. marmoreus</i>	3067.29	CRPPGMVCGFPKPGPYCCSGWCFAVCLPV
Conotoxin-1	<i>C. vexillum</i>	3077.14	DCGEQQQGCYTRPCCPGLHCAAGATGGGSCQP
ViKr92	<i>C. virgo</i>	3081.29	GCLDPGYFCGTPFLGAYCCGGICLIVCIET
Ge6.1	<i>C. generalis</i>	3081.29	GCLDPGYFCGTPFLGAYCCGGICLIVCIET

Based on these results, the molecular weight of PF B indicates that it may be in the O1 family of conotoxins. The results also indicate that it may have about 30-32 amino acids in its sequence. Based on molecular weight alone, though, it is impossible to determine a possible sequence for this peptide.

For PF C (1885 Da), 3 sequences were found in Conoserver that had similar molecular weights. Again, two of them were exactly the same, found in two different cone snails (an A superfamily peptide). The remaining peptide was an M superfamily peptide from *C. litteratus*. All of these peptides came from worm-hunting cone snails. They are listed in Table 7 below. From these results, it can be seen that the Conoserver database does not have any peptides with identical or extremely close molecular weight to PF C. The two different sequences it returned were, however, from superfamilies in which other peptides previously characterized by this laboratory have isolated from *C. brunneus*. Therefore, the results did show some possibility that PF C may be in the A or M superfamily. However, again, with molecular weight data alone, the sequence of PF C was not able to be determined.

Table 7. Conoserver search results for conopeptides with similar MW to PF C (1885 Da).

Name	Cone Snail	MW (Da)	Sequence
Sa1.8	<i>C. sanguinolentus</i>	1874.68	QSCCSTPPCALLYMEMC
Li1.27	<i>C. lividus</i>	1874.68	QSCCSTPPCALLYMEMC
LtIIID	<i>C. litteratus</i>	1876.51	CCDWEWCDELCSCCW

For PF D, two sets of searches were done, one for PF D (2993 Da) and one for PF D (2621 Da). In the search for PF D (2993 Da), 2 different peptides were found in Conoserver with similar molecular weights, shown in Table 8 below. These also came from worm-hunting cone snails, and both were O1 superfamily members. Meanwhile, for PF D (2621 Da), 3 distinct conopeptides with similar molecular weights were found, shown in Table 8 below. This time, 2 of them were from worm-hunters, and 1 was from the molluscivorous *C. textile*. The peptide from *C. distans* was in the O superfamily, and the one from *C. pulicarius* was in the P superfamily.

Table 8. Conoserver search results for conopeptides with similar MW to PF D (2993 Da).

Name	Cone Snail	MW (Da)	Sequence
Ar6.7	<i>C. arenatus</i>	2984.20	QCLPPLHWCNMVDDECCHFCVLLACV
Ac6.2	<i>C. quercinus</i>	2980.16	DCQDSGVVCGFPKPEPHCCSGWCLFVCA

In this case, again, neither of the two peptides that were returned by Conoserver were extremely close in molecular weight to PF D (2993 Da). Therefore, not much information could be drawn from this search, except that it may be possible that this conopeptide could belong to the O superfamily. However, as shown in Table 9 below, two of the results that were obtained for PF D (2621 Da) were very similar in molecular weight (Di6.14 and Pu9.3), suggesting that the 2621-Da conopeptide might be in either the O or P superfamily. Still, the superfamily could not definitively be determined without a closer molecular weight match.

Table 9. Conoserver search results for conopeptides with similar MW to PF D (2621 Da).

Name	Cone Snail	MW (Da)	Sequence
Tx4	<i>C. textile</i>	2610.99	HDSDCCGHLCCAGITCQFTYIPCK
Di6.14	<i>C. distans</i>	2616.00	CLGFGEACLMLYSDCCSYCVGAVCL
Pu9.3	<i>C. pulicarius</i>	2615.89	AGCGGHCLDNSFCPPACSDCSEIYAC

Finally, in the case of PF E, in which the fraction contained one conopeptide that was not identified using previous data by this laboratory, a Conoserver search was done using the molecular weight of the unidentified peptide (1554 Da). Two peptides were found in the search. One was an M conotoxin from *C. litteratus*, and one was an A conotoxin from *C. quercinus*. Both snails are vermivorous. The conopeptides are listed below in Table 10. As can be seen in the table, both sequences that were found were very similar in molecular weight to PF E (1554 Da). Based on this, the results suggested that this PF E peptide may have been either an A or M conotoxin. Since another M conotoxin of similar molecular weight from *C. brunneus* has already been characterized by this laboratory (bru3b; 1746 Da), it might be more probable that PF E was an M conotoxin. However, again, like the other Conoserver-based search results, the superfamily of the peptides could only be guessed at, and the sequence could not be determined at all from molecular weight alone.

Table 10. Conoserver search results for conopeptides with similar MW to PF E (1554 Da).

Name	Cone Snail	MW (Da)	Sequence
LtIIIIC	<i>C. litteratus</i>	1556.43	CCISPACHEECYCC
Qc1.11	<i>C. quercinus</i>	1556.53	GCCSH PACAGNNPDIC

3.2. Glutamate excitotoxicity stroke-related model

3.2.1. ATP assays – primary rat embryonic neuronal cell culture

In general, the primary rat neuronal cell cultures were tested, as described above, in the stroke-related model of induced glutamate excitotoxicity. Several factors may have influenced the luminescence readings, including temperature fluctuations, uneven plating of cells, edge effects, uneven mixing, and general plate reader error. While efforts were made to minimize the impact of these factors on assay results, some error may have occurred. The details of several of the assays are outlined in more depth below, along with the results, shown in Figures 31-34. (All of the peptide fraction concentrations shown below are approximations and were determined using a NanoDrop as described above.)

The results of the first assay that was carried out are shown below in Figure 31. In this test, only taurine (Tau) and two of the conopeptide fractions were compared for their relative neuroprotective effects; glutamate (Glu) only controls were not done in this assay. However, Tau only, peptide fraction only, and cells only controls were done. Also, in this assay, cells which were exposed to more than one test compound (Tau + Glu, or peptide fraction + Glu) were simultaneously treated with them, rather than undergoing pre-treatment. All treated cells were exposed to the test compound(s) for 4 hours.

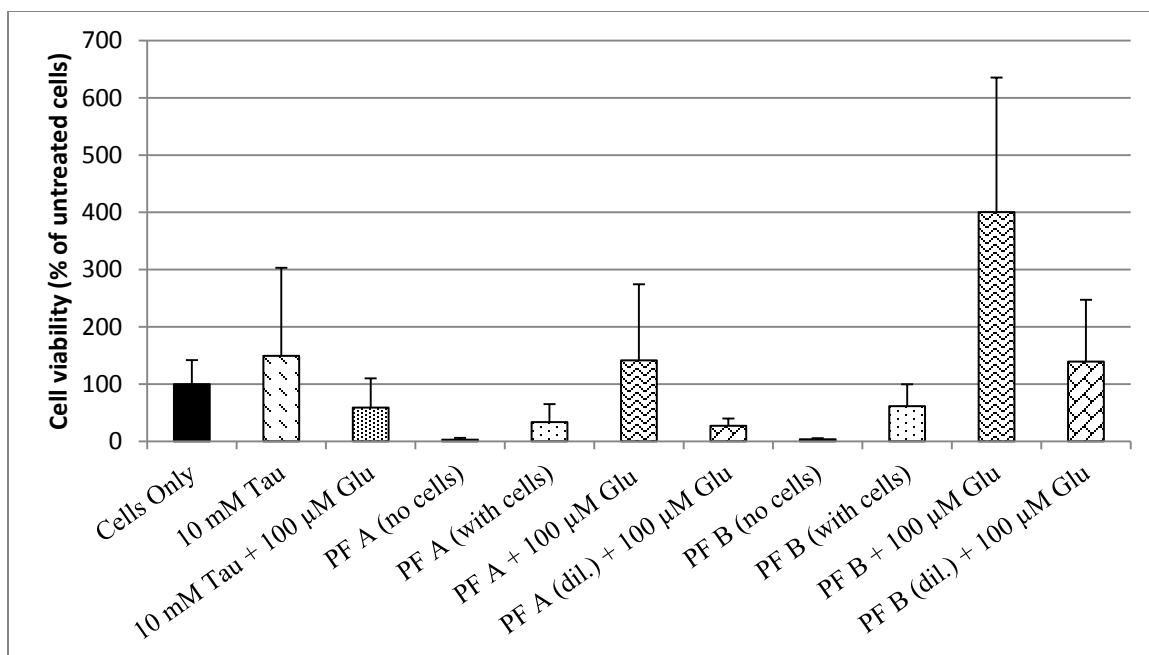


Figure 31. Comparison of the effects of conopeptide fractions A and B vs. taurine on rat primary neuronal cells under induced glutamate excitotoxicity. The approximate peptide fraction concentrations were: PF A (29.720 µg/mL), PF A (100X diluted: 0.2972 µg/mL), PF B (1.9444 µg/mL), and PF B (100X diluted: 0.0194 µg/mL). All the results shown are from wells that contained cells, except where noted (n=3).

As can be seen in the results of the first ATP assay on primary neuronal cells in Figure 31, in the case of the positive control (Tau), as well as PF A + Glu and PF B + Glu, cell viability was even higher (although with large error) than the untreated cells.

Additionally, the 100X diluted PF B showed greater cell viability than untreated cells, showing that even a ng/mL concentration of PF B may have some neuroprotective effect against Glu; however, PF A did not show as much neuroprotective activity at ng/mL concentration. Also shown in this assay was the fact that PF A and PF B (without cells) do not affect the luminescence reading during the assay. Interestingly, it also shows that

when PF A or PF B alone were incubated with cells, the cells did not survive as well as untreated cells. Overall, from this assay, it was determined that both PF A and PF B showed promise as potential neuroprotective agents, and further testing with them was planned.

The next assay that was carried out was designed to optimize the negative (Glu) and positive (Tau) controls. These tests included a series of glutamate only test wells to observe the effects of glutamate alone in the primary neuronal cells. Additionally, several concentrations of taurine only test wells were used, as well as a couple of wells with Tau + Glu (simultaneous treatment). The results are shown in Figure 32 below.

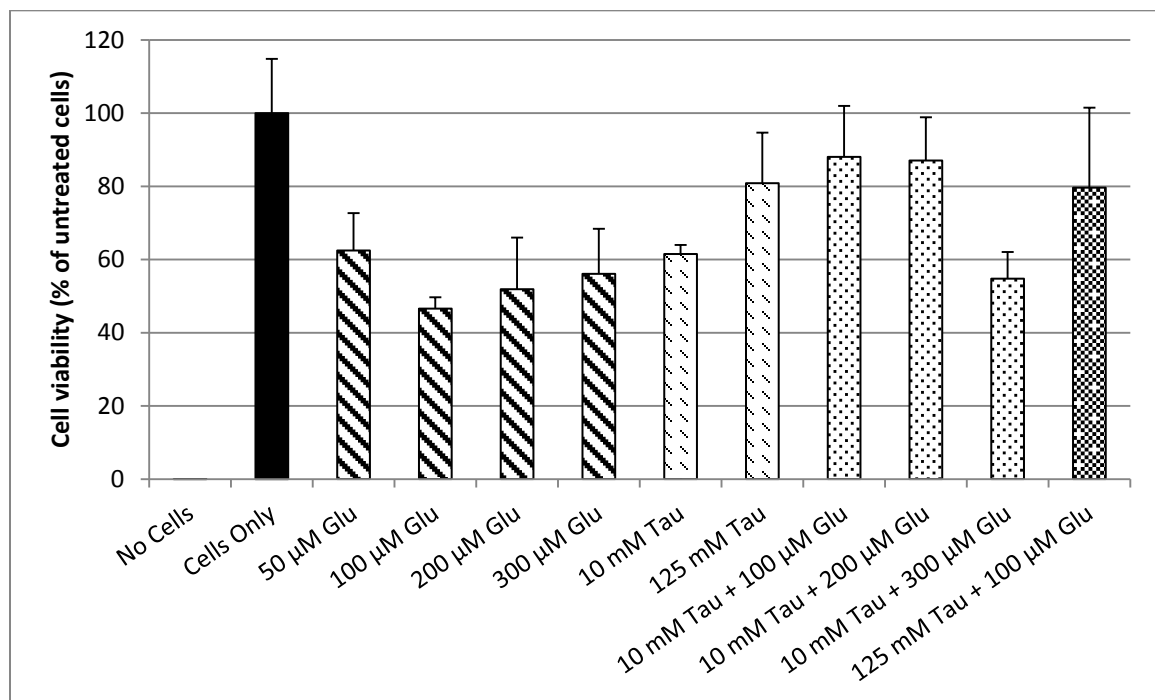


Figure 32. ATP assay of Tau and Glu controls in primary neuronal cells. All the results shown are from wells that contained cells, except where noted (n=3).

As shown in Figure 32 above, the untreated cells gave the highest level of cell viability in this assay. Meanwhile, this assay also showed that wells containing only culture medium gave insignificant luminescence values, so that this could be ruled out as a source of interference in the measurements. There was somewhat of a concentration-dependent level of cell killing by Glu in this assay, in which the general trend was that as Glu concentration increased (including error), the cell viability decreased as expected. Additionally, as Tau concentration increased (from 10 mM to 125 mM), the cell viability increased. Moreover, in the Tau + Glu tests, as Glu concentration increased, the degree to which the Tau aided cell survival gradually decreased from about 90% to about 55% at the usual level of Glu only. And, including error, as Tau concentration increased, its ability to counteract the Glu increased as well. Thus, the results of this assay were very promising and allowed determination of the range of useful concentrations of the controls to use in future assays.

In a later set of tests, peptide fractions A (2533 Da), B (3079 Da), C (1885 Da), and D (2993 Da, 2621 Da) were tested for their neuroprotective effects against induced glutamate excitotoxicity. Again, in this assay, cells which were exposed to more than one test compound (Glu or peptide fraction) were simultaneously treated with them for 4 hours, rather than undergoing pre-treatment. Taurine was not used as a positive control in this assay. The results in Figure 33 below show that the Glu negative controls were somewhat concentration-dependent, including error bars, but did not show a truly gradual decrease in cell viability with increasing Glu concentration. However, many of the cells that were tested with peptide fraction (with or without Glu) gave a clearly higher level of

cell survival than did those treated with Glu alone. Interestingly, again, as seen in earlier ATP assays, the viability of the cells where both peptide fraction + Glu were present, there was greater cell survival than with peptide fraction alone. The peptide fractions that showed the most promising neuroprotective activity in this particular assay were PF A, PF B, and PF D, which all gave improved cell survival against Glu. Even at nM-concentrations PF B and PF D showed promising neuroprotective ability. It may be noted that some of the diluted peptide fractions gave a visibly greater level of cell viability than did their more concentrated counterparts, which may have been due to human error or to the variability of the luminescence reader.

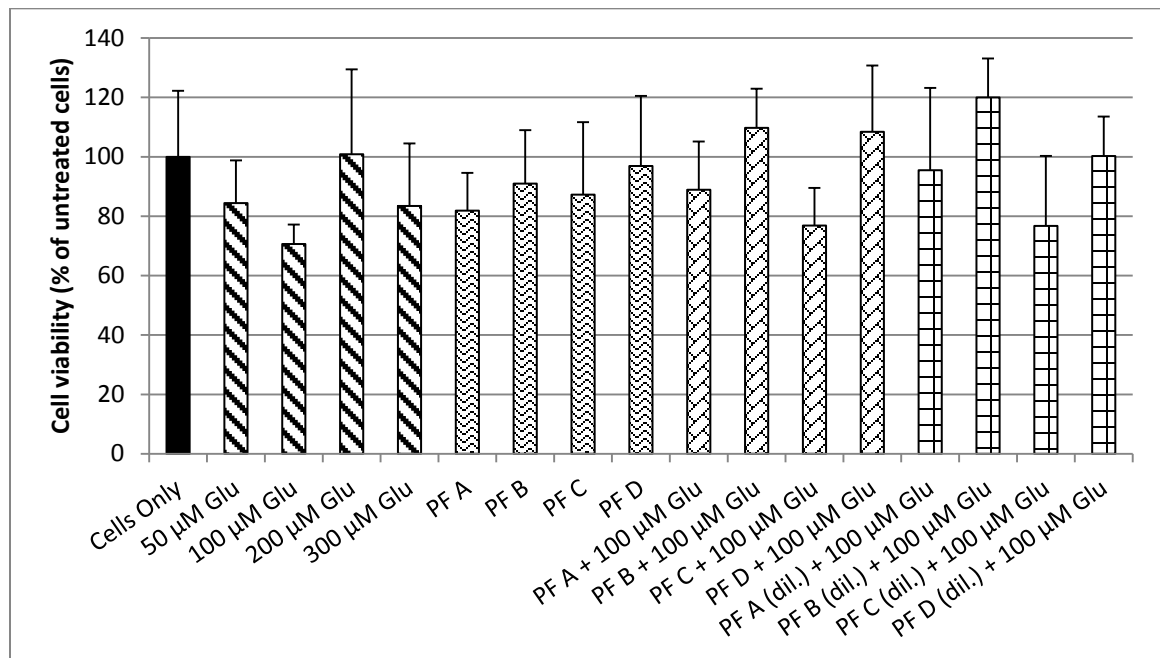


Figure 33. Summary of the ATP assay results for Tau and peptide fractions A-D neuroprotective activity against glutamate insult in primary neuronal cells. The approximate concentrations of the peptide fractions were: A (26.75 µg/mL), B (1.75 µg/mL), C (1.75 µg/mL), D (0.75 µg/mL); and, diluted peptide fractions: A (10X diluted:

2.675 $\mu\text{g/mL}$), B (10X diluted: 0.175 $\mu\text{g/mL}$), C (10X diluted: 0.175 $\mu\text{g/mL}$), and D (10X diluted: 0.075 $\mu\text{g/mL}$) All the results shown are from wells that contained cells (n=3).

After the first few ATP assays, several attempts were made to improve the positive and negative control results and reproducibility to observe steadier and more reproducible concentration dependence for cell killing with Glu. For this reason, only one more set of assays was done with the primary cell cultures in which all six peptide fractions were tested. In this set of experiments, cells exposed to more than one test compound (Tau + Glu, or peptide fraction + Glu) were pre-treated with Tau or peptide fraction for 1 hour before exposure to Glu for 4 hours. The results of these experiments are shown in Figure 34. As can be seen, the Glu controls did not behave as expected, with an increase in cell viability as the concentration of Glu increased. Additionally, Tau did not seem to save the cells treated Glu (10 μM), but it did seem to save the cells that were treated with Glu (100 μM). Moreover, a similar pattern was observed with the peptide fractions used to pre-treat cells. In fact, in the 100 μM Glu-treated cells, all six peptide fractions showed promising neuroprotective activity versus the Glu-only treated cells.

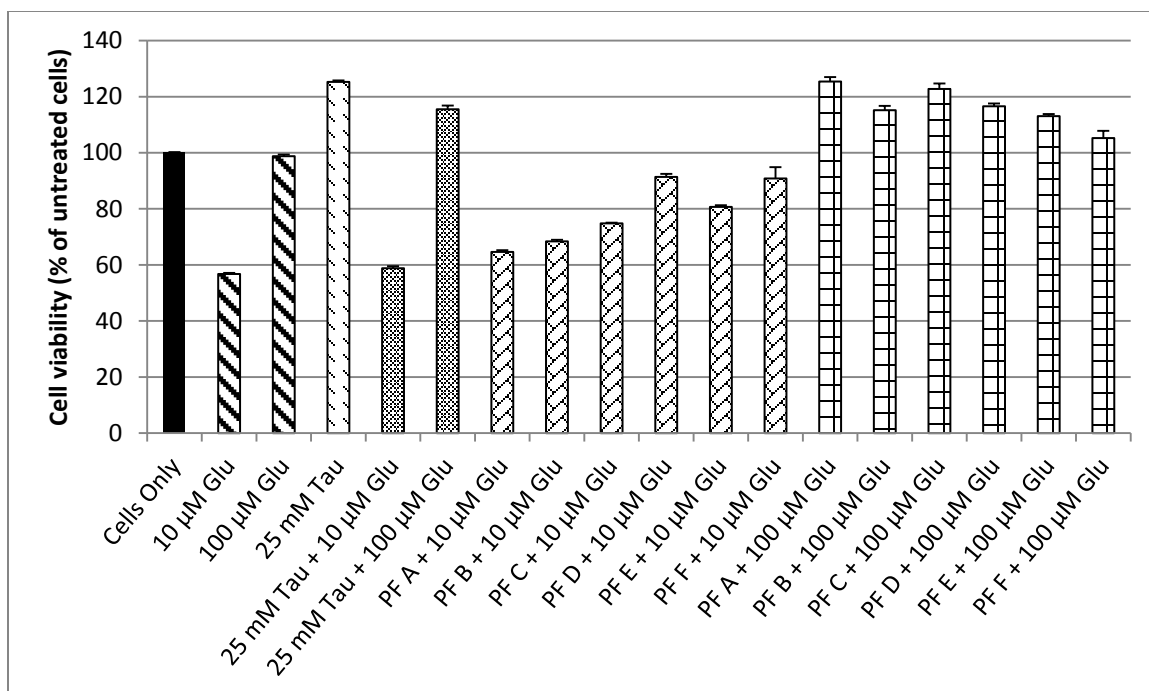


Figure 34. Summary of assay results of Tau and peptide fractions A-F. The approximate concentrations of the peptide fractions were: A (13.375 µg/mL), B (0.875 µg/mL), C (0.875 µg/mL), D (0.375 µg/mL), E (0.500 µg/mL), and F (5.625 µg/mL) neuroprotective activity against glutamate insult in primary, with Tau only and Glu only controls. All the results shown are from wells that contained cells (n=3).

3.2.2. ATP assays – PC12 cell culture

In addition to carrying out ATP assays on the primary neuronal cell cultures from rat embryonic brain cells, similar testing was done using PC12 rat pheochromocytoma cells. These ATP assays were carried out as described above, and with the same possible sources of error. Below in Figures 35-38 are several of the preliminary results obtained from the PC12 ATP assays, with a few details specific to each one.

In the first couple of rounds of testing, the goal was to determine optimum concentrations to use for the positive (Tau) and negative (Glu) controls again, as was

done for the primary cells. As shown below in Figure 35, PC12 cells were tested with a range of concentrations of Glu in the presence or absence of Tau, with a pre-treatment time of between 12 or 24 hours. Between 10 and 20 mM Glu, there was about 50 % cell death. However, the concentration of Tau that was used was clearly not high enough to counteract the Glu, even at 24 hours of pre-treatment with Tau.

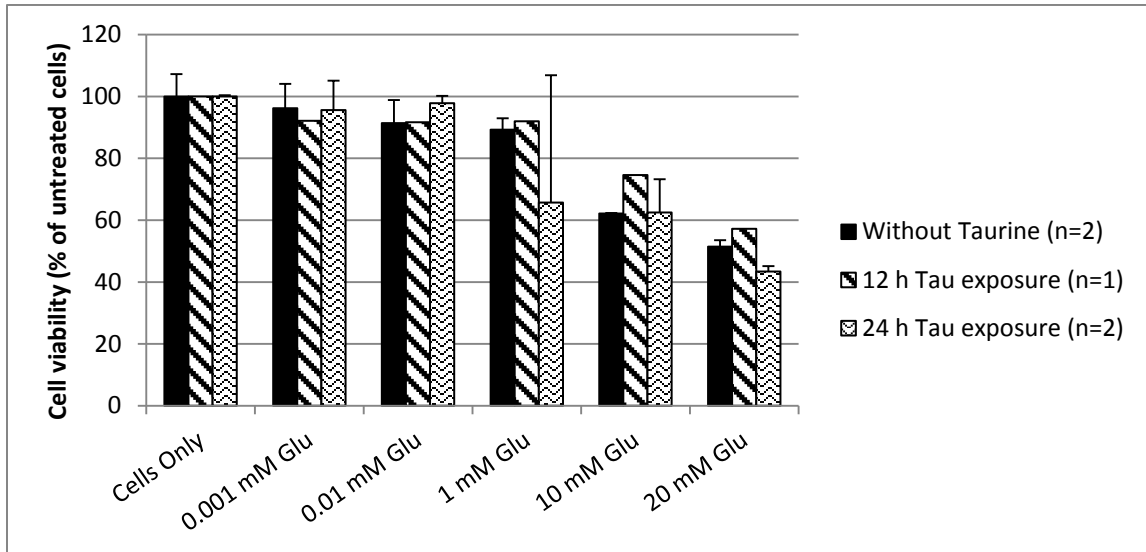


Figure 35. ATP assay of Tau and Glu controls in PC12 cells. The concentration of Tau was 10 mM. All the results shown are from wells that contained undifferentiated PC12 cells (2.8×10^5 cells/well).

After this first assay, it was clear that further testing was needed to more accurately determine the optimum concentration and pre-treatment time of Tau to use as a positive control, so that another series of tests were run in which Tau pre-treatment was done for 1 hour, 2 hours, 6 hours, or 12 hours. These results are shown below in Figure 36. The best results were observed for Tau pre-treatment time of 6 hours, with a concentration range of 10 mM Tau to 100 mM Tau yielding the highest luminescence

values (and thus cell viability). On the other hand, for the cells treated with Tau for 1 hour, as concentration of Tau increased, cell viability decreased, and a similar pattern was observed for 2-hour exposure to Tau. The results for 12-hour exposure to Tau showed a fairly concentration-independent luminescence output, with only the 50 mM Tau giving a luminescent signal close to that of 6-hour exposure.

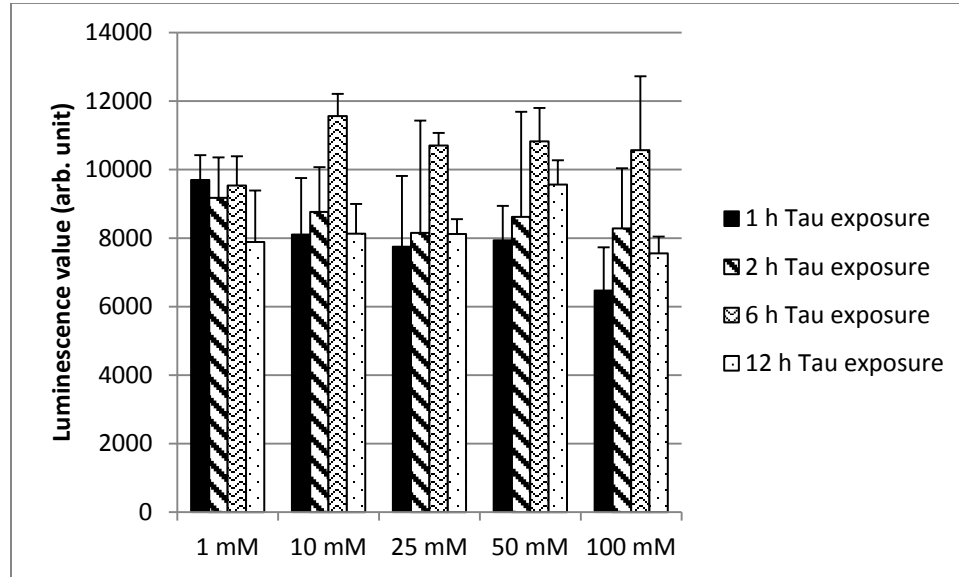


Figure 36. ATP assay to determine the optimum concentration and pre-treatment time of Tau for future use as the positive control in PC12 cell tests (n=3). All the results shown are from wells that contained undifferentiated PC12 cells (2.8×10^5 cells/well).

To view the same results in a different way, each set of results for each exposure time was calculated as a percentage of the 1 mM Tau results for that exposure time in Figure 37. In this way, it can be seen that, again exposure to Tau for 1 to 2 hours resulted in lower cell viability, while exposure for 12 hours gave much better cell viability (even higher than the 6-hour exposure at 50 mM Tau), but that again 6 hours exposure generally gave the highest cell viability.

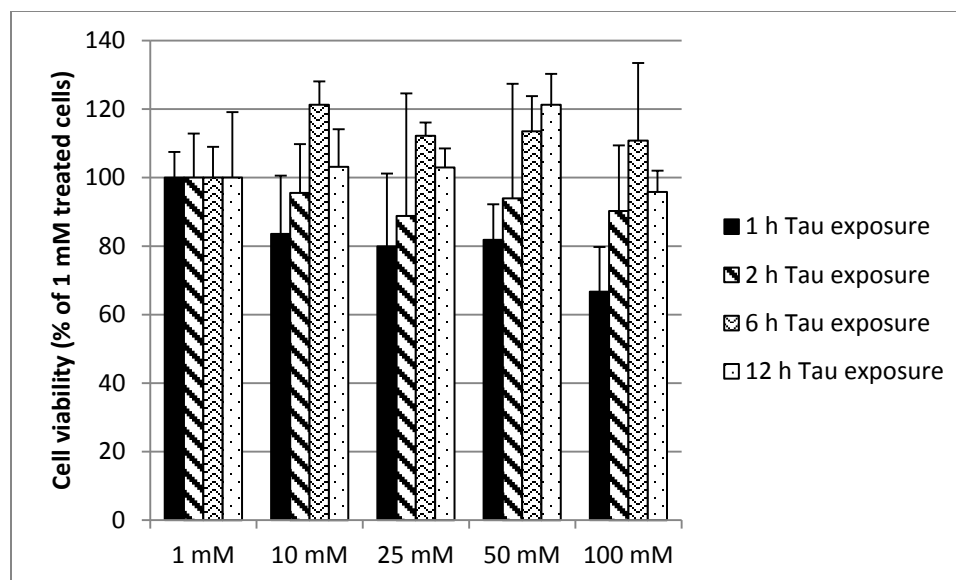


Figure 37. ATP assay to determine the optimum concentration and pre-treatment time of Tau for future use as the positive control in PC12 cell tests, in terms of cell viability (n=3). All the results shown are from wells that contained undifferentiated PC12 cells (2.8×10^5 cells/well).

Finally, one set of ATP assays was done using peptide fractions to test for their neuroprotective activity against induce glutamate excitotoxicity in PC12 cells. This time, all six peptide fractions were tested, including PF A (2533 Da), PF B (3079 Da), PF C (1885 Da), PF D (2993 Da; 2621 Da), PF E (2357 Da; 1554 Da), and PF F (2127 Da). In peptide fraction tests, the cells were pre-treated with peptide for 6 hours, followed by exposure to Glu (10 mM) for 6 hours; Tau only cells were treated with Tau for 6 hours as well. The results of this set of ATP assays are shown below in Figure 38. The Tau positive controls and the Glu negative controls did not give results as expected. As Tau concentration increased, cell viability should also have increased, but instead decreased; moreover, as the Glu concentration increased, cell viability should have decreased, but

instead increased. Therefore, the results obtained for the peptide test fractions could not be conclusively interpreted; however, it did seem that some of the peptide fractions (PF A and PF B) may have shown some potential at counteracting glutamate excitotoxicity in PC12 cells.

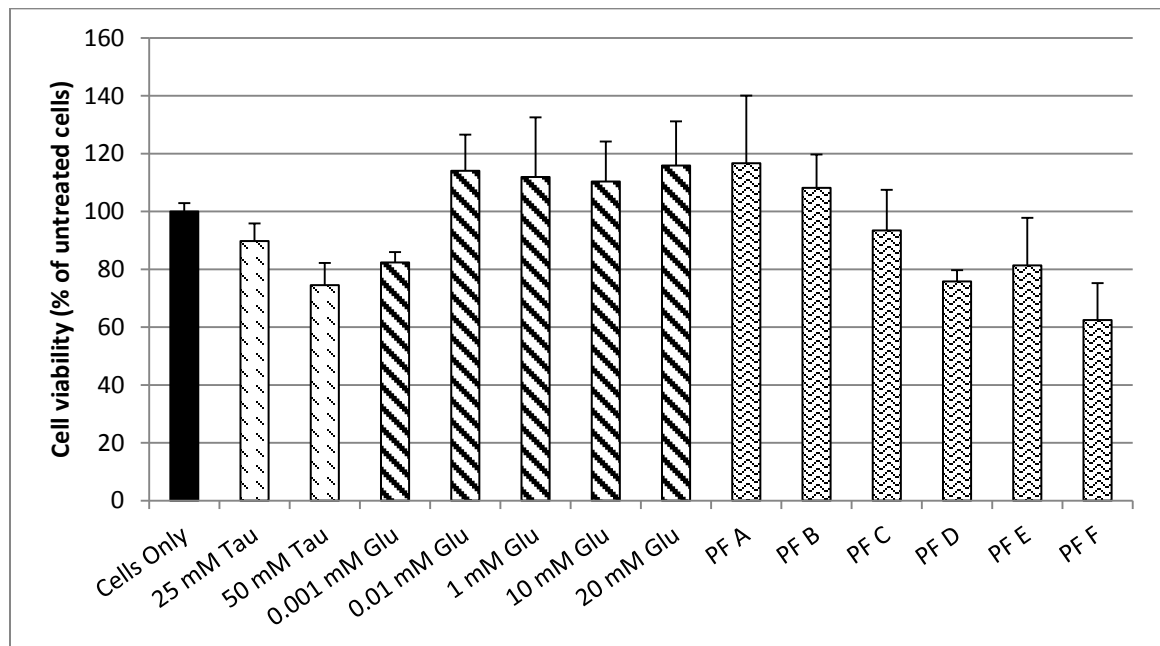


Figure 38. ATP assay of peptide fractions against glutamate insult in PC12 cells. For all of the peptide fraction tests, Glu (10 mM) was used. The peptide fraction concentrations were: PF A (53.50 $\mu\text{g/mL}$), PF B (3.50 $\mu\text{g/mL}$), PF C (3.50 $\mu\text{g/mL}$), PF D (1.50 $\mu\text{g/mL}$), PF E (2.0 $\mu\text{g/mL}$), and PF F (22.5 $\mu\text{g/mL}$). All the results shown are from wells that contained undifferentiated PC12 cells (2.8×10^5 cells/well) ($n=3$).

3.2.3. Western blot analysis

Several pro-survival and pro-apoptosis protein levels were also examined in this stroke-related model of induced glutamate excitotoxicity, using Western blot analysis as described above. A few of the Western blot results are shown below in Figures 39 and 40.

For each of them, the concentrations of peptide fractions used were the same: PF A (12.159 $\mu\text{g/mL}$), PF B (0.795 $\mu\text{g/mL}$), PF C (0.795 $\mu\text{g/mL}$), PF D (0.341 $\mu\text{g/mL}$), PF E (0.455 $\mu\text{g/mL}$), and PF F (5.114 $\mu\text{g/mL}$). The concentration of Glu used was 300 μM . Cells were pre-treated with peptide for 4 hours, followed by Glu exposure for 4 hours.

Below in Figure 39 is a Western blot, using PC12 cells, in which the levels of the anti-apoptotic Bcl-2 and Akt were tested. In addition, GAPDH (the enzyme used in the 6th step of glycolysis) was used as an internal control. The GAPDH level was about the same for all of the treated cells; however, it seemed to be highest for PF A and lowest for PF D, which was closest to the level in untreated cells. The level of Akt was also noticeably much higher in the case of PF A, but for all of the other peptide fractions, it was about the same, or even lower (PF D) than in the case of Glu (negative control). At the same time, the Bcl-2, while not very clear, did seem to show increased levels of expression in cells treated with PF A, PF B, PF C, and PF F, with the highest density apparently for PF F.

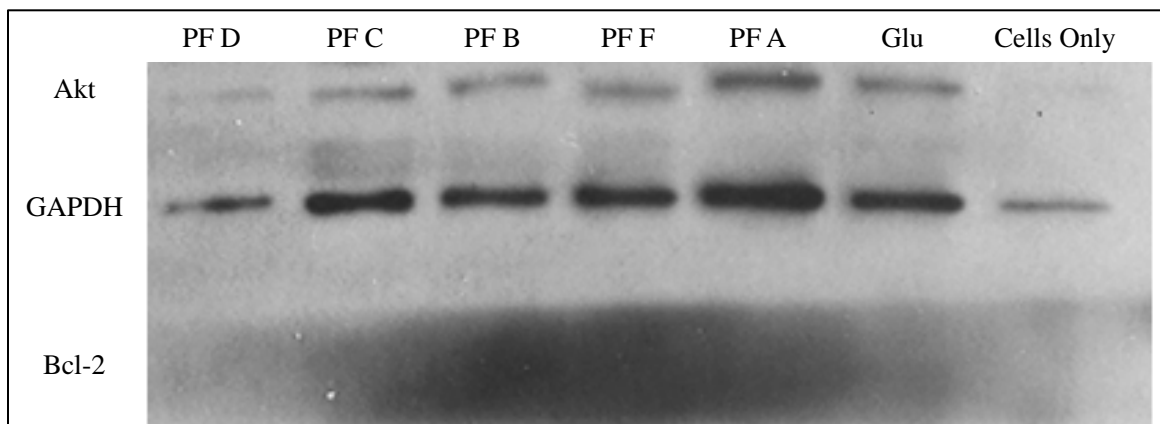


Figure 39. Western blot of the pro-survival markers Akt and Bcl-2 in PC12 cells pre-treated with peptide fractions and exposed to Glu.

Western blot analysis was also done using primary neuronal cells in a similar fashion. All of the test conditions were the same as those for the PC12 cells described above. In the two sets of results shown below in Figure 40, the anti-apoptotic Bcl-2 was again tested, along with caspase-12 (pro-apoptotic), calpain (pro-apoptotic Ca^{2+} -dependent protease) [94], GRP78 (ER chaperone upregulated during UPR), and GAPDH (again used as an internal control).

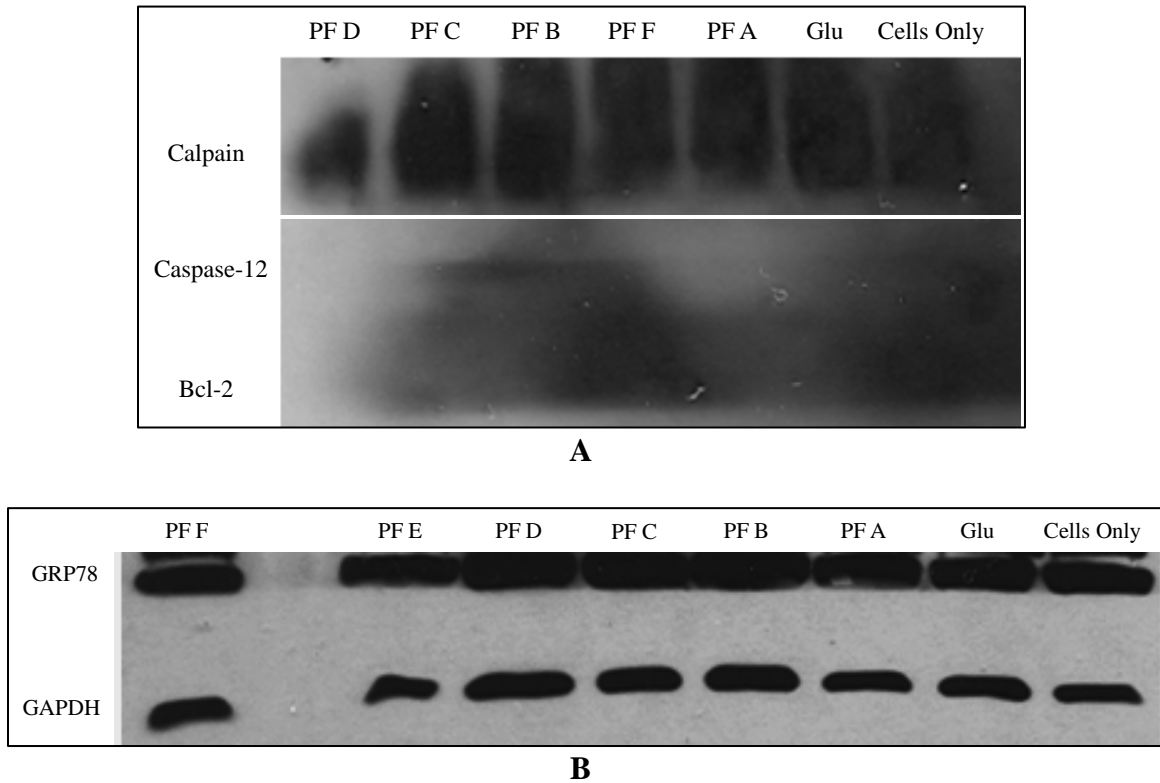


Figure 40. Western blot of several markers of ER stress and apoptosis in rat primary neuronal cells pre-treated with peptide fractions and exposed to Glu. A) Pro-survival Bcl-2, and pro-apoptotic calpain and caspase-12. B) GAPDH internal control and UPR-upregulated ER chaperone GRP78.

In Figure 40A, it was observed again as in the PC12 cells above, that the Bcl-2 signal was not very clear at all; however, a higher density did seem to be there for PF F. A much clearer result was seen for caspase-12, which was significantly lower for PF A and PF D versus Glu. Meanwhile, the level of calpain seemed to be highest for PF B and PF C (which also contained higher levels of caspase-12), and was lowest for PF D. In Figure 40B, GRP78 and GAPDH expression appeared to be very similar for all of the test conditions. Overall, these results indicated that PF A, PF D, and PF F may have some possible neuroprotective effect.

4. CONCLUSIONS

To summarize, 6 peptide fractions were isolated from *C. brunneus*, a vermivorous marine cone snail. Molecular weight data was obtained for all of the peptides, and NMR data was obtained for three of the peptides (PF A, PF C, and PF F). Three peptides were identified based on previous data obtained by this laboratory. These were bru9a (PF A; 2533 Da), bru3a (PF F; 2127 Da), and an α -conotoxin (PF E; 2357 Da). The identity of bru9a was confirmed by nearly identical NMR data to that obtained previously in this laboratory, while bru3a and the α -conotoxin were identified based on molecular weight. Meanwhile, 5 of the peptides were not identified.

Overall, the biological testing with the peptide fractions in rat primary neuronal cells and PC12 cells gave a very preliminary view of possible neuroprotective activity of some of the peptide fractions against induced glutamate excitotoxicity. However, a major problem with the ATP assays was that the Glu (negative) and Tau (positive) controls were never quite standardized, so that many of the results obtained were inconclusive. Several approaches were attempted to try to solve this issue, including standardizing the number of cells/well more precisely and very carefully controlling the concentrations of compounds in the medium. It may have been possible that some of the cells present in the well-plates were simply insensitive to Glu excitotoxicity, and so, did not give concentration-dependent results as expected. Additionally, it may have sometimes been the case that incubation times were not optimized to be able to observe cell death (via

long-term ER stress-induced apoptosis), but rather the pro-survival initial phase of the UPR.

On the other hand, the results obtained from the Western blot analysis were more promising in that they were fairly consistent for each individual peptide fraction, so that it could be concluded that PF A, PF D, and PF F may have more neuroprotective potential than the other peptides. This would be an extremely exciting finding, since the molecular target of PF A (bru9a, the most abundant conotoxin found in *C. brunneus* venom), as well as PF F (bru3a) and possibly the unidentified PF D, have never been determined. Their potential as inhibitors of Glu-induced excitotoxicity suggests that they may act as antagonists of an important receptor or receptors in that process, such as a Glu receptor or Ca^{2+} receptor.

One factor to take into consideration in future research will be the concentration of peptide fractions. For all of the assays done in the current study, the relative levels of peptide fractions used in testing were not standardized; instead, they were used as isolated from the venom, in an effort to simulate most closely the activity of the components of the cone snail venom at their physiological levels in nature. In the future, a range of standardized concentrations of the isolated peptides should be tested. In conclusion, more research will be required to structurally characterize the isolated peptides more thoroughly and to more conclusively determine the extent and mode of action of their potential neuroprotective agency against induced glutamate excitotoxicity in this stroke-related model.

5. REFERENCES

1. Catterall WA. (1992). Cellular and molecular biology of voltage-gated calcium channels. *Physiol. Rev.*, **72**(Suppl 4): S15-S48.
2. Brush DE. Chapter 116. Marine envenomation. *Goldfrank's Toxicologic Emergencies*, Vol. 8, Flomenbaum NE, Goldfrank LR, Hoffman RS, Howland MA, and Lewin NA, Eds. New York, NY: McGraw-Hill; 2006.
3. Lewis RJ, Dutertre S, Vetter I, and Christie MJ. (2012). *Conus* venom peptide pharmacology. *Pharmacol. Rev.*, **64**(2): 259-298.
4. Olivera BM. (2002). *Conus* venom peptides: Reflections from the biology of clades and species. *Annu. Rev. Ecol. Syst.*, **33**: 25-47.
5. Terlau H and Olivera BM. (2004). *Conus* venoms: A rich source of novel ion channel-targeted peptides. *Physiol. Rev.*, **84**(1): 41-68.
6. Marí F and Fields GB. (2003). Conopeptides: Unique pharmacological agents that challenge current peptide methodologies. *Chim. Oggi*, **21**: 43-48.
7. Kaas Q, Westermann JC, and Craik DJ. (2010). Conopeptide characterization and classifications: An analysis using ConoServer. *Toxicon*, **55**(8): 1491-1509.
8. Terlau H, Shon K, Grilley M, Stocker M, Stuhmer W, and Olivera BM. (1996). Strategy for rapid immobilization of prey by a fish-hunting cone snail. *Nature*, **381**(6578): 148-151.

9. Jacob RB and McDougal OM. (2010). The M-superfamily of conotoxins: A review. *Cell. Mol. Life Sci.*, **67**(1): 17-27.
10. McDougal OM and Poulter CD. (2004). Three-dimensional structure of the mini-M conotoxin mr3a. *Biochemistry*, **43**(2): 425-429.
11. Corpuz GP, Jacobsen RB, Jimenez EC, Watkins M, Walker C, Colledge C, Garrett JE, McDougal O, Li W, Gray WR, Hillyard DR, Rivier J, McIntosh JM, Cruz LJ, and Olivera BM. (2005). Definition of the M-conotoxin superfamily: Characterization of novel peptides from molluscivorous *Conus* venoms. *Biochemistry*, **44**(22): 8176-8186.
12. Olivera BM. (1997). E.E. Just Lecture, 1996: *Conus* venom peptides, receptor and ion channel targets, and drug design: 50 million years of neuropharmacology. *Mol. Biol. of the Cell*, **8**(11): 2101-2109.
13. Pflueger FC. (2008). Isolation and characterization of novel conopeptides from the marine cone snail: *Conus brunneus*. Thesis (Ph.D.)--Florida Atlantic University.
14. Furie B, Bouchard BA, and Furie BC. (1999). Vitamin-K dependent biosynthesis of γ -carboxyglutamic acid. *Blood*, **93**(6): 1798-1808.
15. Olivera BM, Hillyard DR, Marsh M, and Yoshikami D. (1995). Combinatorial peptide libraries in drug design: Lessons from venomous cone snails. *Trends in Biotechnology*. **13**(10): 422-426.
16. Czerweic E, Kalume DE, Roepstorff P, Hambe B, Furie B, Furie BC, and Stenflo J. (2006). Novel γ -carboxyglutamic acid-containing peptides from the venom of *Conus textile*. *The FEBS Journal*. **273**(12): 2779-2788.

17. Mejia M, Heghinian MD, Busch A, Armishaw CJ, Marí F, and Godenschwege TA. (2010). A novel approach for *in vivo* screening of toxins using the *Drosophila* giant fiber circuit. *Toxicon*, **56**(8): 1398-1407.
18. Williams JA, Day M, and Heavner JE. (2008). Ziconotide: An updated review. *Expert Opin. Pharmacother.*, **9**(9): 1575-1583.
19. Clark RJ, Jensen J, Nevin ST, Callaghan BP, Adams DJ, and Craik DJ. (2010). The engineering of an orally active conotoxin for the treatment of neuropathic pain. *Angew Chem. Int. Ed.*, **49**(37): 6545-6548.
20. Clark RJ, Akcan M, Kaas Q, Daly NL, and Craik DJ. (2012). Cyclization of conotoxins to improve their biopharmaceutical properties. *Toxicon*, **59**(4): 446-455.
21. Shon K-J, Olivera BM, Watkins M, Jacobsen RB, Gray WR, Floresca CZ, Cruz LJ, Hillyard DR, Brink A, Terlau H, and Yoshikami D. (1998). μ -Conotoxin PIIIA, a new peptide for discriminating among tetrodotoxin-sensitive Na channel subtypes. *J. Neurosci.*, **18**(12): 4473-4481.
22. Twede VD, Miljanich G, Olivera BM, and Bulaj G. (2009). Neuroprotective and cardioprotective conopeptides: An emerging class of drug leads. *Curr. Opin. Drug Discov. Devel*, **12**(2): 231-239.
23. Lloyd-Jones D, Adams R, Carnethon M, de Simone G, Ferguson TB, Flegal K, Ford E, Furie K, Go A, Greenlund K, Haase N, Hailpern S, Ho M, Howard V, Kissela B, Kittner S, Lackland D, Lisabeth L, Marelli A, McDermott M, Meigs J, Mozaffarian D, Nichol G, O'Donnell C, Roger V, Rosamond W, Sacco R, Sorlie P, Stafford R, Steinberger J, Thom T, Wasserthiel-Smoller S, Wong N, Wylie-Rosett J, and Hong

- Y. (2009). Heart disease and stroke statistics--2009 update: A report from the American Heart Association statistics committee and stroke statistics subcommittee. *Circulation*, **119**(3): 480-486 (e21-e181).
24. National Heart, Lung, and Blood Institute. *Incidence and Prevalence: 2006 Chart Book on Cardiovascular and Lung Diseases*. Bethesda, MD: National Institutes of Health; 2006. 138p.
25. National Center for Health Statistics, Centers for Disease Control, and Prevention. *Compressed Mortality File: Underlying Cause of Death, 1979 to 2009*. Atlanta, GA: Centers for Disease Control and Prevention; 2013.
26. Asplund K, Stegmayr B, and Peltonen M. Chapter 64. From the twentieth to the twenty-first century: A public health perspective on stroke. *Cerebrovascular Disease Pathophysiology, Diagnosis, and Management*, Vol. 2, Ginsberg MD and Bogousslavsky J, Eds. Malden, MA: Blackwell Science; 1998.
27. Kelley-Hayes M, Beiser A, Kase CS, Scaramucci A, d'Agostino RB, and Wolf PA. (2003). The influence of gender and age on disability following ischemic stroke: The Framingham study. *J. Stroke Cerebrovasc. Dis.*, **12**(3): 119 –126.
28. Rosamond WD, Folsom AR, Chambless LE, Wang CH, McGovern PG, Howard G, Copper LS, and Shahar E. (1999). Stroke incidence and survival among middle-aged adults: 9-year follow-up of the atherosclerotic risk in communities (ARIC) cohort. *Stroke*. **30**(4): 736 –743.
29. Konishi M, Iso H, Komachi Y, Iida M, Shimamoto T, Jacobs DR, Jr., Terao A, Baba S, Sankai T, and Ito M. (1993). Association of serum total cholesterol, different types

- of stroke, and stenosis distribution of cerebral arteries. The Akita Pathology Study. *Stroke*, **24**: 954-964.
30. Hossmann KA. (1994). Glutamate-mediated injury in focal cerebral ischemia: The excitotoxin hypothesis revised. *Brain Pathol.*, **4**(1): 23-36.
 31. Da'valos A, Shuaib A, and Wahlgren NG. (2000). Neurotransmitters and pathophysiology of stroke: Evidence for the release of glutamate and other transmitters/mediators in animals and humans. *J. Stroke Cerebrovasc. Dis.*, **9**(6): 2-8.
 32. Liang D, Bhatta S, Gerzanich V, and Simard JM. (2007). Cytotoxic edema: Mechanisms of pathological cell swelling. *Neurosurg. Focus*, **22**(5): E2.
 33. Lipton P. (1999). Ischemic cell death in brain neurons. *Physiol. Rev.*, **79**:1431- 1568.
 34. Danbolt NC. (2001). Glutamate uptake. *Prog. Neurobiol.*, **65**(1): 1-105.
 35. Siesjö BK, Agardh C-D, and Bengtsson F. (1989). Free radicals and brain damage. *Cerebrovasc. Brain Metab. Rev.*, **1**:165–211.
 36. Hoehn-Berlage M, Hossmann KA, Busch E, Eis M, Schmitz B, and Gyngell ML. (1997). Inhibition of nonselective cation channels reduces focal ischemic injury of rat brain. *J. Cereb. Blood Flow Metab.*, **17**(5): 534-542.
 37. Xiong ZG, Zhu XM, Chu XP, Minami M, Hey J, Wei WL, MacDonald JF, Wemmie JA, Price MP, Welsh MJ, and Simon RP. (2004). Neuroprotection in ischemia: Blocking calcium-permeable acid-sensing ion channels. *Cell*, **118**(6): 687-698.
 38. Sweeney MI, Yager JY, Walz W, and Juurlink BH. (1995). Cellular mechanisms involved in brain ischemia. *Can. J. Physiol Pharmacol.*, **73**(11): 1525-1535.

39. Kahle KT, Simard JM, Staley KJ, Nahed BV, Jones PS, and Sun D. (2009). Molecular mechanisms of ischemic cerebral edema: Role of electroneutral ion transport. *Physiology (Bethesda)*, **24**: 257-265.
40. Choi DW and Rothman SM. (1990). The role of glutamate neurotoxicity in hypoxic ischemic neuronal death. *Annu. Rev. Neurosci.*, **13**:171–182.
41. Kristian T and Siesjö BK. (1998). Calcium in ischemic cell death. *Stroke*, **29**(3): 705-718.
42. White BC, Sullivan JM, DeGracia DJ, O’Neil BJ, Neumar RW, Grossman LI, Rafols JA, and Krause GS. (2000). Brain ischemia and reperfusion: Molecular mechanisms of neuronal injury. *J. Neurol. Sci.*, **179**(S1-2): 1-33.
43. Baumann O and Walz BB. (2001). Endoplasmic reticulum of animal cells and its organization into structural and functional domains. *Int. Rev. Cytol.*, **205**: 149–214.
44. Lai E, Teodoro T, and Volchuk A. (2007). Endoplasmic reticulum stress: Signaling the unfolded protein response. *Physiol.*, **22**: 193-201.
45. Ito D, Tanaka K, Suzuki S, Dembo T, Kosakai A, and Fukuuchi Y. (2001). Up-regulation of the Ire1-mediated signaling molecule, BiP, in ischemic rat brain. *Neuroreport*, **12**(18): 4023–4028.
46. Mouw G, Zechel JL, Gamboa J, Lust WD, Selman WR, and Ratcheson RA. (2003). Activation of caspase-12, an endoplasmic reticulum resident caspase, after permanent focal ischemia in rat. *Neuroreport*, **14**(2): 183–186.

47. Paschen W, Aufenberg C, Hotop S, and Mengesdorf T. (2003). Transient cerebral ischemia activates processing of xbp1 messenger RNA indicative of endoplasmic reticulum stress. *J. Cereb. Blood Flow Metab.*, **23**(4): 449–461.
48. Harding HP, Zhang Y, Bertolotti A, Zeng H, and Ron D. (2000). PERK is essential for translational regulation and cell survival during the unfolded protein response. *Mol. Cell*, **5**(5): 897–904.
49. Wang XZ, Harding HP, Zhang Y, Jolicoeur EM, Kuroda M, and Ron D. (1998). Cloning of mammalian Ire1 reveals diversity in the ER stress responses. *EMBO J.*, **17**(19): 5708–5717.
50. Yoshida H, Haze K, Yanagi H, Yura T, and Mori K. (1998). Identification of the cis acting endoplasmic reticulum stress response element responsible for transcriptional induction of mammalian glucose-regulated proteins. Involvement of basic leucine zipper transcription factors. *J. Biol. Chem.*, **273**(50): 33741–33749.
51. Szegezdi E, D'Angela, O'Mahoney ME, Logue SE, Mylotte LA, O'Brien T, and Samali A. (2006). ER stress contributes to ischemia-induced cardiomyocyte apoptosis. *Biochem. Biophys. Res. Commun.*, **349**(4): 1406–1411.
52. Nickson P, Toth A, and Erhardt P. (2007). PUMA is critical for neonatal cardiomyocyte apoptosis induced by endoplasmic reticulum stress. *Cardiovasc. Res.*, **73**(1): 48–56.
53. Kaufman RJ. (2002) Orchestrating the unfolded protein response in health and disease. *J. Clin. Invest.*, **110**(10): 1389–1398.

54. Ji C and Kaplowitz N. (2004). Hyperhomocysteinemia, endoplasmic reticulum stress, and alcoholic liver injury. *World J. Gastroentero.*, **10**(12): 1699-1708.
55. Oyadomari S and Mori M. (2004). Roles of CHOP/GADD153 in endoplasmic reticulum stress. *Cell Death Differ.*, **11**(4): 381–389.
56. McCullough KD, Martindale JL, Klotz LO, Aw TY, and Holbrook NJ. (2001). Gadd153 sensitizes cells to endoplasmic reticulum stress by downregulating Bcl2 and perturbing the cellular redox state. *Mol. Cell Biol.*, **21**(4): 1249 –1259.
57. Puthalakath H, O'Reilly LA, Gunn P, Lee L, Kelly PN, Huntington ND, Hughes PD, Michalak EM, McKimm-Breschkin J, Motoyama N, Gotoh T, Akira S, Bouillet P, and Strasser A. (2007). ER stress triggers apoptosis by activating BH3-only protein Bim. *Cell*, **129**(7): 1337–1349.
58. Nishitoh H, Saitoh M, Mochida Y, Takeda K, Nakano H, Rothe M, Miyazono K, and Ichijo H. (1998). ASK1 is essential for JNK/SAPK activation by TRAF2. *Mol. Cell*, **2**(3): 389–395.
59. Urano F, Wang X, Bertolotti A, Zhang Y, Chung P, Harding HP, and Ron D. (2000). Coupling of stress in the ER to activation of JNK protein kinases by transmembrane protein kinase IRE1. *Science*, **287**(5453): 664–666.
60. Davis RJ. (2000). Signal transduction by the JNK group of MAP kinases. *Cell*, **103**(2): 239–252.
61. Szegezdi E, Logue SE, Gorman AM, and Samali A. (2006). Mediators of endoplasmic reticulum stress-induced apoptosis. *EMBO J.*, **7**(9): 880-885.

62. Berge E, Abdelnoor M, Nakstad PH, and Sandset PM. (2000). Low molecular-weight heparin versus aspirin in patients with acute ischaemic stroke and atrial fibrillation: A doubleblind randomised study. *Lancet*, **355**(9211): 1205 – 1210.
63. Huang Y, Huang YL, Lai B, Zheng P, Zhu YC, and Yao T. (2007). Raloxifene acutely reduces glutamate-induced intracellular calcium increase in cultured rat cortical neurons via inhibition of high-voltage-activated calcium current. *Neuroscience*, **147**(2): 334-341.
64. Cheng H-Y, Hsieh M-T, Wu C-R, Tsai F-H, Lu T-C, Hsieh C-C, Li W-C, Lin Y-T, and Peng W-H. (2008). Schizandrin protects primary cultures of rat cortical cells from glutamate-induced excitotoxicity. *J. Pharmacol. Sci.*, **107**(1): 21-31.
65. Chen WQ, Jin H, Nguyen M, Carr J, Lee YJ, Hsu CC, Faiman MD, Schloss JV, and Wu JY. (2001). Role of taurine in regulation of intracellular calcium level and neuroprotective function in cultured neurons. *J. Neurosci. Res.*, **66**(4): 612-619.
66. Pan C, Gupta A, Prentice H, and Wu J-Y. (2010). Protection of taurine and granulocyte colony-stimulating factor against excitotoxicity induced by glutamate in primary cortical neurons. *J. Biomed. Sci.*, **17**(Suppl 1): S18.
67. Pan C, Prentice H, Price AL, and Wu J-Y. (2012). Beneficial effect of taurine on hypoxia- and glutamate-induced endoplasmic reticulum stress pathways in primary neuronal culture. *Amino Acids*. **43**(2): 845-855.
68. Khan H, Banigesh A, Baziani A, Todd KG, Miyashita H, Eweida M, and Shuaib A. (2000). The role of taurine in neuronal protection following transient global forebrain ischemia. *Neurochem. Research*, **25**(2): 217–223.

69. Shyu W-C, Lin S-Z, Lee C-C, Liu DD, and Li H. (2006). Granulocyte colony stimulating factor for acute ischemic stroke: A randomized controlled trial. *CMAJ*, **174**(7): 927-933.
70. Weaver CH, Buckner CD, Longin K, Appelbaum FR, Rowley S, Lilleby K, Miser J, Storb R, Hansen JA, and Bensinger W. (1993). Syngeneic transplantation with peripheral blood mononuclear cells collected after the administration of recombinant human granulocyte colony-stimulating factor. *Blood*, **82**(7): 1981-1984.
71. Hartung T. (1998). Anti-inflammatory effects of granulocyte colony-stimulating factor. *Curr. Opin. Hematol.*, **5**: 221–225.
72. Schabitz WR, Kollmar R, Schwaninger M, Juettler E, Bardutzky J, Scholzke MN, Sommer C, and Schwab S. (2003). Neuroprotective effect of granulocyte colony stimulating factor after focal cerebral ischemia. *Stroke*, **34**(3): 745–751.
73. Solaroglu I, Tsubokawa T, Cahill J, Zhang JH. (2006). Anti-apoptotic effect of granulocyte colony stimulating factor after focal cerebral ischemia in the rat. *Neuroscience*, **143**(4): 965–974.
74. Meuer K, Pitzer C, Teismann P, Krüger C, Göricke B, Laage R, Lingor P, Peters K, Schlachetzki JC, Kobayashi K, Dietz GP, Weber D, Ferger B, Schäbitz WR, Bach A, Schulz JB, Bähr M, Schneider A, and Weishaupt JH. (2006). Granulocyte-colony stimulating factor is neuroprotective in a model of Parkinson's disease. *J. Neurochem.*, **97**(3): 675– 686.

75. Tsai KJ, Tsai YC, and Shen CK. (2007). G-CSF rescues the memory impairment of animal models of Alzheimer's disease. *J. Exp. Med.*, **204**(6):1273–1280.
76. Shyu WC, Lin SZ, Yang HI, Tzeng YS, Pang CY, Yen PS, and Li H. (2004). Functional recovery of stroke rats induced by granulocyte colony-stimulating factor-stimulated stem cells. *Circulation*, **110**(13):1847–1854.
77. Lee S-T, Chu K, Jung K-H, Ko S-Y, Kim E-H, Sinn DI, Lee YS, Lo EH, Kim M, and Roh JK. (2005). Granulocyte colony-stimulating factor enhances angiogenesis after focal cerebral ischemia. *Brain Res.*, **1058**(1-2): 120–128.
78. Li Y, Chen J, Wang L, Lu M, and Chopp M. (2001). Treatment of stroke in rat with intracarotid administration of marrow stromal cells. *Neurology*, **56**(12): 1666–1672.
79. Hald J and Jacobsen E. (1948). A drug sensitizing the organism to ethyl alcohol. *Lancet*, **2**(6539): 1001–1004.
80. Madan A, Parkinson A, and Faiman MD. (1995). Identification of the human and rat P450 enzymes responsible for the sulfoxidation of S-methyl N,N-diethylthiolcarbamate (DETC-ME). The terminal step in the bioactivation of disulfiram. *Drug Metab. Dispos.*, **23**(10): 1153–1162 .
81. Nagendra NS, Faiman MD, Davis K, Wu JY, Newby X, and Schloss JV. (1997). Carbamoylation of brain glutamate receptors by disulfiram metabolite. *J. Bio. Chem.*, **272**: 24247-24251.

82. Jin L, Davis MR, Hu P, and Baillie TA. (1994). Identification of novel glutathione conjugates of disulfiram and diethyldithiocarbamate in rat bile by liquid chromatography-tandem mass spectrometry. Evidence for metabolic activation of disulfiram in vivo. *Chem. Res. Toxicol.*, **7**(4): 526–533.
83. Huxtable RJ. (1992). Physiological actions of taurine. *Physiol. Rev.*, **72**(1): 101-163.
84. Schaffer SW and Azuma J. (1992). Myocardial physiological effects of taurine and their significance. *Adv. Exp. Biol. Med.*, **315**: 105-120.
85. Schaffer S, Solodushko V, and Azuma J. (2000). Taurine-deficient cardiomyopathy: Role of phospholipids, calcium and osmotic stress. *Adv. Exp. Med. Biol.*, **483**: 57-69.
86. Wu H, Jin Y, Wei J, Jin H, Sha D, and Wu JY. (2005). Mode of action of taurine as a neuroprotector. *Brain Res.*, **1038**(2): 123-131.
87. Leon R, Wu H, Jin Y, Wei J, Buddhala C, Prentice H, and Wu J-Y. (2009). Protective function of taurine in glutamate-induced apoptosis in cultured neurons. *J. Neurosci. Res.*, **87**(5): 1185–1194.
88. Chepkova AN, Doreulee N, Yanovsky Y, Mukhopadhyay D, Haas HL, and Sergeeva OA. (2002). Long-lasting enhancement of corticostriatal neurotransmission by taurine. *Eur. J. Neurosci.*, **16**(8): 1523-1530.
89. Song H, Kim H, Park T, and Lee DH. (2009). Characterization of myogenic differentiation under endoplasmic reticulum stress and taurine treatment. *Adv. Exp. Med. Biol.*, **643**: 253-261.

90. Shuaib A. (2003). The role of taurine in cerebral ischemia: Studies in transient forebrain ischemia and embolic focal ischemia in rodents. *Adv. Exp. Med. Biol.*, **526**: 421-423.
 91. Schurr A, Tseng MT, West CA, and Rigor BM. (1987). Taurine improves the recovery of neuronal function following cerebral hypoxia: An *in vitro* study. *Life Sci.*, **40**: 2059-2066.
 92. Lehmann A, Hagberg H, Nyström B, Sandberg M, and Hamberger A. (1985). *In vivo* regulation of extracellular taurine and other neuroactive amino acids in the rabbit hippocampus. *Prog. Clin. Biol. Res.*, **179**: 289-311.
 93. Sun GC, Wang D, and Tao C. (2000). Effects of taurine on the levels of prostaglandins in brain tissue during cerebral ischemia/reperfusion in rats. *Chinese Pharm. J.*, **35**: 815-817.
 94. Sharma AK and Rohrer B. (2004). Calcium-induced calpain mediates apoptosis via caspase-3 in a mouse photoreceptor cell line. *J. Biol. Chem.*, **279**: 35564-35572.
- Additional resources:
- Becker S and Terlau H. (2008). Toxins from cone snails: properties, applications and biotechnological production. *Appl. Microbiol. Biotechnol.*, **79**: 1-9.
- Halai R and Craik DJ. (2009). Conotoxins: Natural product drug leads. *Nat. Prod. Rep.*, **26**: 526-536.
- Jin Y, Wu H, Cohen EM, Wei J, Jin H, Prentice H, and Wu J-Y. (2007). Genistein and daidzein induce neurotoxicity at high concentrations in primary rat neuronal cultures. *J. Biomed. Sci.*, **14**: 275-284.

- Kaas Q, Yu R, Jin AH, Dutertre S, and Craik DJ. (2012). ConoServer: Updated content, knowledge, and discovery tools in the conopeptide database. *Nucleic Acids Res.*, **40**: D325-D330.
- Kaas Q, Westermann J-C, and Craik DJ. (2010). Conopeptide characterization and classifications: An analysis using ConoServer. *Toxicon.*, **55**(8): 1491-1509.
- Lewis RJ and Garcia ML. (2003). Therapeutic potential of venom peptides. *Drug Discov.*, **2**: 1-15.
- Majno G and Joris I. (1995). Apoptosis, oncosis, and necrosis. An overview of cell death. *Am. J. Pathol.*, **146**(1): 3-15.
- Olivera BM. (May 2006). "Part 2: How a Fish Hunting Snail Captures its Prey". iBioSeminars. <<http://ibioseminars.org/lectures/chemicalbiologybiophysics/baldomero-olivera/baldomero-olivera-part-2.html>>.
- Olivera BM. (May 2006). "Part 3: Conus Peptide Genes a 'Drug Development Program'". iBioSeminars. <<http://www.ibioseminars.org/lectures/chemicalbiologybiophysics/baldomero-olivera/baldomero-olivera-part-3.html>>.
- Pegorini S, Braida D, Verzoni C, Guerini-Rocco C, Consalez GG, Croci L, and Sala M. (2005). Capsaicin exhibits neuroprotective effects in a model of transient global cerebral ischemia in Mongolian gerbils. *Br. J. Pharmacol.*, **144**(5): 727-735.
- Puillandre N, Koua D, Favreau P, Olivera BM, and Stocklin R. (2012). Molecular phylogeny, classification and evolution of conopeptides. *J. Mol. Evol.*, **74**(5-6): 297-309.

- Raffa RB. (2010). Diselenium, instead of disulfide, bonded analogs of conotoxins: Novel synthesis and pharmacotherapeutic potential. *Life Sciences*, **87**: 451-456.
- Yan Y, Dempsey R, Flemmer A, Forbush B, and Sun D. (2003). Inhibition of Na(+)-K(+)-Cl(-) cotransporter during focal cerebral ischemia decreases edema and neuronal damage. *Brain Res.*, **961**(1): 22-31.